American Journal of Pathology, Vol. 167, No. 1, July 2005

Tumorigenesis and Neoplastic Progression

Uniform Overexpression and Rapid Accessibility of $\alpha_5\beta_1$ Integrin on Blood Vessels in Tumors

Patricia Parsons-Wingerter,* Ian M. Kasman,* Scott Norberg,* Anette Magnussen,* Sara Zanivan,* Alberto Rissone,* Peter Baluk,* Cecile J. Favre,* Ursula Jeffry,† Richard Murray,† and Donald M. McDonald*

From the Department of Anatomy, Cardiovascular Research Institute, Comprehensive Cancer Center, University of California, San Francisco; and Protein Design Labs, Incorporated,† Fremont, California*

Integrin $\alpha_5\beta_1$ is among the proteins overexpressed on tumor vessels and is a potential target for diagnostics and therapeutics. Here, we mapped the distribution of $\alpha_5\beta_1$ integrin in three murine tumor models and identified sites of expression that are rapidly accessible to intravascular antibodies. When examined by conventional immunohistochemistry, $\alpha_5\beta_1$ integrin expression was strong on most blood vessels in RIP-Tag2 transgenic mouse tumors, adenomatous polyposis coli (*apc*) mouse adenomas, and implanted MCa-IV mammary carcinomas. Expression increased during malignant progression in RIP-Tag2 mice. However, immunoreactivity was also strong in normal pancreatic ducts, intestinal smooth muscle, and several other sites. To determine which sites of expression were rapidly accessible from the bloodstream, we intravenously injected anti-$\alpha_5\beta_1$ integrin antibody and 10 minutes to 24 hours later examined the amount and distribution of labeling. The injected antibody strongly labeled tumor vessels at all time points but did not label most normal blood vessels or gain access to pancreatic ducts or intestinal smooth muscle. Intense vascular labeling by anti-$\alpha_5\beta_1$ integrin antibody co-localized with the uniform CD31 immunoreactivity of tumor vessels and contrasted sharply with the patchy accumulation of nonspecific IgG at sites of leakage. This strategy of injecting antibodies revealed the uniform overexpression and rapid accessibility of $\alpha_5\beta_1$ integrin on tumor vessels and may prove useful in assessing other potential therapeutic targets in cancer. *(Am J Pathol 2005, 167:193–211)*

The vasculature of tumors is an attractive therapeutic target. Promising clinical evidence documents the beneficial effects of angiogenesis inhibitors in some types of cancer.[1,2] Multiple processes are involved. Inhibition of angiogenesis can stop tumor growth, destruction of tumor vessels can lead to tumor regression, and normalization of tumor vessels can augment the delivery of chemotherapeutics and the effect of irradiation.[3–8] Substances can be directed to the vasculature of tumors by targeting molecules overexpressed on tumor vessels. Such targets have been identified by gene profiling of endothelial cells isolated from tumors,[9] *in vivo* phage display,[10,11] as well as other ways. Among the best characterized vascular targets are integrins.[12–16]

The accessibility of vascular targets is governed by their cellular location and relationship to the endothelial barrier. In normal vessels, the barrier function of the endothelium restricts the extravasation of macromolecules, limiting access to pericytes and the abluminal surface of endothelial cells. In tumors, defects in the endothelial monolayer and other abnormalities make blood vessels leakier than their normal counterparts.[17–20] Vascular leakiness makes it possible to reach targets in tumors that would normally be isolated by the endothelial barrier. However, not all tumor vessels are equally leaky, leakiness is heterogeneous along individual tumor vessels, and the amount of leakage is limited by the high interstitial fluid pressure in tumors.[19,21,22] The effective-

Supported in part by the University of California (BioSTAR grants S98-50 and 99-10067), the National Institutes of Health (grants HL-24136 and HL-59157 from the National Heart, Lung, and Blood Institute; P50-CA90270 from the National Cancer Institute), the AngelWorks Foundation, the Vascular Mapping Project (to D.M.M.), and by Microgravity Science, NASA Glenn Research Center (to P.P.-W.).

P.P.-W. and I.M.K. contributed equally to this work.

Accepted for publication March 10, 2005.

Present address of P.P.-W.: Microgravity Science Division, NASA Glenn Research Center, Cleveland, OH 44135; I.M.K.: Genentech, Inc., South San Francisco, CA 94080; S.Z. and A.R.: Department of Oncological Sciences, University of Turin, Italy; C.F.: Integra LifeSciences, San Diego, CA 92121; U.J.: Chiron Corp., Emeryville, CA 94608.

Address reprint requests to Donald M. McDonald, Department of Anatomy, S1363, University of California, 513 Parnassus Ave., San Francisco, CA 94143-0452. E-mail: dmcd@itsa.ucsf.edu.

ness of molecular targets in tumors for macromolecular therapeutics in the bloodstream is thus determined by their amount of expression, cellular distribution, and accessibility.

Integrin $\alpha_5\beta_1$ and its ligand fibronectin have been found to be overexpressed in blood vessels of human and mouse tumors.[13] The oncofetal isoform of fibronectin with an extra domain B (ED-B) is up-regulated in tumor vessels and is being explored as a diagnostic and therapeutic target.[23] Selective antagonists targeted to $\alpha_5\beta_1$ integrin reverse tumor growth in preclinical models[13,14,24] and have entered clinical trials.[25] Selective inhibitors of $\alpha_5\beta_1$ integrin are thought to lead to endothelial cell apoptosis by anoikis and other mechanisms.[13,14]

The present study sought to obtain a better understanding of the distribution of $\alpha_5\beta_1$ integrin expression and to identify which sites are accessible to antibodies in the bloodstream. Specifically, we 1) compared the cellular distribution of $\alpha_5\beta_1$ integrin in tumors and normal organs, 2) examined the accessibility of $\alpha_5\beta_1$ integrin on tumor blood vessels to antibodies in the bloodstream, and 3) determined the extent and uniformity of expression of $\alpha_5\beta_1$ integrin on blood vessels in different mouse tumor models and during tumor progression.

Our approach was first to use conventional immunohistochemistry to determine the distribution of $\alpha_5\beta_1$ integrin in mice. Next, we tested the accessibility of the integrin by injecting the same anti-$\alpha_5\beta_1$ integrin antibody intravenously and examining sites of binding 10 minutes to 24 hours later. Using these two approaches, we compared the distribution and accessibility of $\alpha_5\beta_1$ integrin in pancreatic islet tumors in RIP-Tag2 transgenic mice,[26] intestinal adenomas in adenomatous polyposis coli (*apc*) mice,[27,28] implanted MCa-IV mouse mammary carcinomas,[20] and 11 normal organs. Immunoreactivity of $\alpha_5\beta_1$ integrin was co-localized with the endothelial cell marker CD31 (PECAM-1) to determine the uniformity of integrin expression in vascular networks.[29] Fluorescence and confocal microscopic imaging, confirmed by fluorescence measurements, showed that $\alpha_5\beta_1$ integrin was uniformly expressed in blood vessels of all three tumor models, increased in expression during tumor progression, and, unlike the integrin in most normal organs, was rapidly accessible to antibodies in the bloodstream.

Materials and Methods

Murine Tumor Models

Three tumor models were studied. 1) Pancreatic islet tumors derived from β-cells in islets of Langerhans were studied in RIP-Tag2 transgenic mice with a C57BL/6 background.[26,30] Tumor-bearing RIP-Tag2 mice from our colony were identified by genotyping tail tip DNA and studied at 9 to 14 weeks of age.[20,30] Tumors in individual RIP-Tag2 mice ranged from hyperplastic islets—little larger than normal islets—to carcinomas several millimeters in diameter. 2) Intestinal adenomas in adenomatous polyposis coli (*apc*) mice, which have ~35 adenomas by 16 weeks of age, vary in size but are arrested at about the same stage of progression.[27,28] Adenomas in *apc* mice (C57BL/6J-*Apc*^{Min}/J; Jackson Laboratory, Bar Harbor, MA) were studied at 16 to 21 weeks of age. 3) Cubes (2 mm) of MCa-IV mouse mammary carcinomas (gift from Rakesh Jain, Massachusetts General Hospital, Harvard University, Boston, MA) were implanted under the dorsal skin of male C3H mice (25 to 30 g) and studied 2 to 3 weeks later when the tumors were 5 to 9 mm in diameter.[18,31] This highly reproducible tumor model was developed to visualize the tumor vasculature in a dorsal skinfold chamber in a setting not influenced by hormonal changes during the female estrus cycle.[18] This approach was used in the present experiments so the data could be related to those obtained previously.[20] Similar results were obtained when the tumors were implanted in mammary fat pads of female mice. Normal organs were studied in adult wild-type C57BL/6 mice. All experimental procedures were approved by the University of California, San Francisco, Institutional Animal Care and Use Committee.

Intravenous Injection of Antibodies

Mice, anesthetized by intramuscular injection of ketamine (87 mg/kg) and xylazine (13 mg/kg), received an injection of: 1) purified rat anti-mouse integrin α_5 subunit antibody (50 μg per mouse or ~2 mg/kg, anti-CD49e, clone 5H10-27, no. 553318; BD Biosciences PharMingen, San Diego, CA); 2) purified nonspecific IgG (50 μg, rat IgG2a,κ monoclonal immunoglobulin isotype standard, clone R35-95, no. 553926; BD PharMingen); or 3) sterile saline (100 μl, 0.9% NaCl; Abbott Laboratories, North Chicago, IL) into a femoral or tail vein. To determine the extent of labeling of tumor vasculature, some mice received an injection of anti-$\alpha_5\beta_1$ integrin antibody in combination with hamster monoclonal anti-CD31 antibody (50 μg, clone 2H8; Chemicon, Temecula, CA). Antibodies were diluted in sterile saline to final volume of 50 to 100 μl. Mice injected with saline were used for conventional immunohistochemistry.

The specificity of the antibody used to mark $\alpha_5\beta_1$ integrin is important to the meaningfulness of our results. This well-characterized rat anti-mouse monoclonal antibody was originally identified by T. Springer at Harvard University, where it was known as clone MRF5 (5H10) (*http://cbr.med.harvard.edu/investigators/springer/lab/*). The antibody is now available commercially as anti-CD49e antibody clone 5H10-27 from BD Biosciences Pharmingen (*http://www.bdbiosciences.com*), where specificity for α_5 integrin has been tested by flow cytometry and cell binding assays. Because α_5 integrin subunits pair solely with β_1 integrin subunits, we treated anti-α_5 integrin antibody as if it binds exclusively to $\alpha_5\beta_1$ integrin and designate it as such. The antibody has been reported to have blocked fibronectin binding *in vitro*, but function-blocking actions on endothelial cells or angiogenesis have not been demonstrated *in vitro* or *in vivo*.[32,33]

Vascular Perfusion Fixation and Immunohistochemistry

In most experiments antibodies, IgG, or saline circulated for 10 minutes before perfusion of fixative. In studies of the kinetics of accumulation in tumors, anti-$\alpha_5\beta_1$ integrin antibody or IgG circulated for 10 minutes or 1, 6, or 24 hours. The chest was opened rapidly, and the vasculature was perfused for 3 minutes at a pressure of 120 mmHg with fixative [4% paraformaldehyde in phosphate-buffered saline (PBS), pH 7.4; Sigma, St. Louis, MO] from an 18-gauge cannula inserted into the aorta via an incision in the left ventricle. The right atrium was incised to create an exit route. After the perfusion, tissues were immersed in fixative for 1 hour, rinsed with PBS, infiltrated overnight with 30% sucrose in PBS at 4°C, embedded in OCT (Sakura Finetek, Torrance, CA) and frozen at −80°C. Tissue sections were cut with a cryostat (Microm International GmbH, Walldorf, Germany) at a thickness of 100 μm, unless otherwise indicated, and dried on glass slides (Superfrost Plus; Fisher Scientific, Pittsburgh, PA). After removal of the OCT, sections were blocked and permeabilized by incubation in 5% normal goat serum containing 1% Triton X-100 in PBS for 3 hours.

Sections from anti-$\alpha_5\beta_1$ integrin or IgG-injected mice were incubated for 12 to 15 hours in hamster anti-mouse CD31 antibody (monoclonal antibody 2H8; kind gift of Dr. William Muller, Department of Pathology, Cornell University Medical College, New York, NY or monoclonal 1398Z antibody, Chemicon). Sections used for conventional immunohistochemistry were incubated for 12 to 15 hours in CD31 antibody in combination with anti-$\alpha_5\beta_1$ integrin antibody or nonspecific IgG used for intravenous injections. Primary antibodies (initial concentration, 1 mg/ml) were diluted 1:200 or 1:400 with PBS containing 5% normal goat serum and 1% Triton X-100.[30] The identity of smooth muscle cells in intestinal villi was confirmed by staining with purified mouse monoclonal anti-α-smooth muscle actin antibody (Cy3-conjugated, no. C6198, Sigma).[30] Sections were rinsed several times with PBS and then incubated for 6 hours in a combination of two secondary antibodies: Cy3-labeled anti-rat antibody for $\alpha_5\beta_1$ integrin and fluorescein isothiocyanate-labeled anti-hamster antibody for CD31 (Jackson ImmunoResearch, West Grove, PA). Secondary antibodies were diluted 1:200 or 1:400 with PBS containing 1% normal goat serum and 0.3% Triton X-100. Sections were mounted with Vectashield (Vector Laboratories, Burlingame, CA) for fluorescence microscopic imaging. Tissue sections from mice that had intravenous injections of both anti-$\alpha_5\beta_1$ integrin and anti-CD31 antibodies were incubated for 6 hours in a mixture of Cy3-labeled anti-rat and fluorescein isothiocyanate-labeled anti-hamster secondary antibodies (Jackson ImmunoResearch), rinsed with PBS, and mounted with Vectashield.

Fluorescence Imaging

Tissue sections were examined with a Zeiss Axiophot fluorescence microscope equipped with single, dual, and triple fluorescence filters and a low-light, externally cooled, three-chip charge-coupled device (CCD) camera (480 × 640 pixel RGB color images, CoolCam; SciMeasure Analytical Systems, Atlanta, GA) and with a Zeiss LSM 510 confocal microscope (Carl Zeiss MicroImaging, Inc., Thornwood, NY) with argon, helium-neon, and UV lasers (512 × 512 or 1024 × 1024 pixel RGB color images). The amount of immunoreactivity in tissue sections prepared 10 minutes after intravenous injection of anti-$\alpha_5\beta_1$ integrin antibody or nonspecific IgG was quantified in digital images of 100-μm-thick cryostat sections stained with Cy3-labeled anti-rat secondary antibody. For fluorescence measurements, RGB color images were captured with the CCD camera (×10 objective, ×1 Optovar, tissue region 960 × 1280 μm), and then the red (Cy3) channel was converted to an 8-bit gray scale image (fluorescence intensity range, $0 < 255$) for analysis using ImageJ v.1.29 (*http://rsb.info.nih.gov/ij*).

Immunofluorescence Measurements

Pilot studies revealed that, when section thickness, magnification, and microscope filters were held constant, subtle differences in immunohistochemical staining and CCD camera gain were the technical factors that contributed the most variability to the fluorescence intensity of images. Tissue staining was, therefore, standardized by simultaneously processing all slides in a particular data set (RIP-Tag2 tumors, *apc* tumors, or MCa-IV tumors). CCD camera gain was standardized as follows. First, after the brightest section (reference specimen) of a data set was identified, a digital image was acquired with the CCD camera. Next, the distribution of pixel fluorescence intensities of the image was displayed using the histogram function of Adobe Photoshop (Adobe Systems Inc., San Jose, CA). Camera gain was then adjusted, another image acquired, and the process repeated until the intensity histogram for the reference specimen image was well distributed, as judged by pixels throughout the entire intensity range with few or no pixels at maximal intensity of 255. When the camera gain for the reference specimen was optimized, the entire data set of images was acquired using this gain.

Pancreatic islet tumors in RIP-Tag2 mice were classified by their diameters in tissue sections as small (< 500 μm), medium ($500 < 1000$ μm), or large (≥ 1000 μm), which approximately correspond to stage of tumor progression.[26] Digital images of three to four tumors of each size in one or more sections of pancreas from each mouse were acquired. Regions of interest (ROI), defined by tissue boundaries identified by their vascular pattern in specimens stained for $\alpha_5\beta_1$ integrin and CD31 immunoreactivities, were outlined with the freehand tool of ImageJ (Figures 1 and 2). The ROI of normal islets and small and medium size tumors was completely included in a single image. Large tumors, which exceeded the size of a single image, were sampled by acquiring three images at 4, 8, and 12 o'clock around the tumor, each image representing one ROI. Fluorescence intensities of the pixels within the ROI were then recorded with ImageJ.

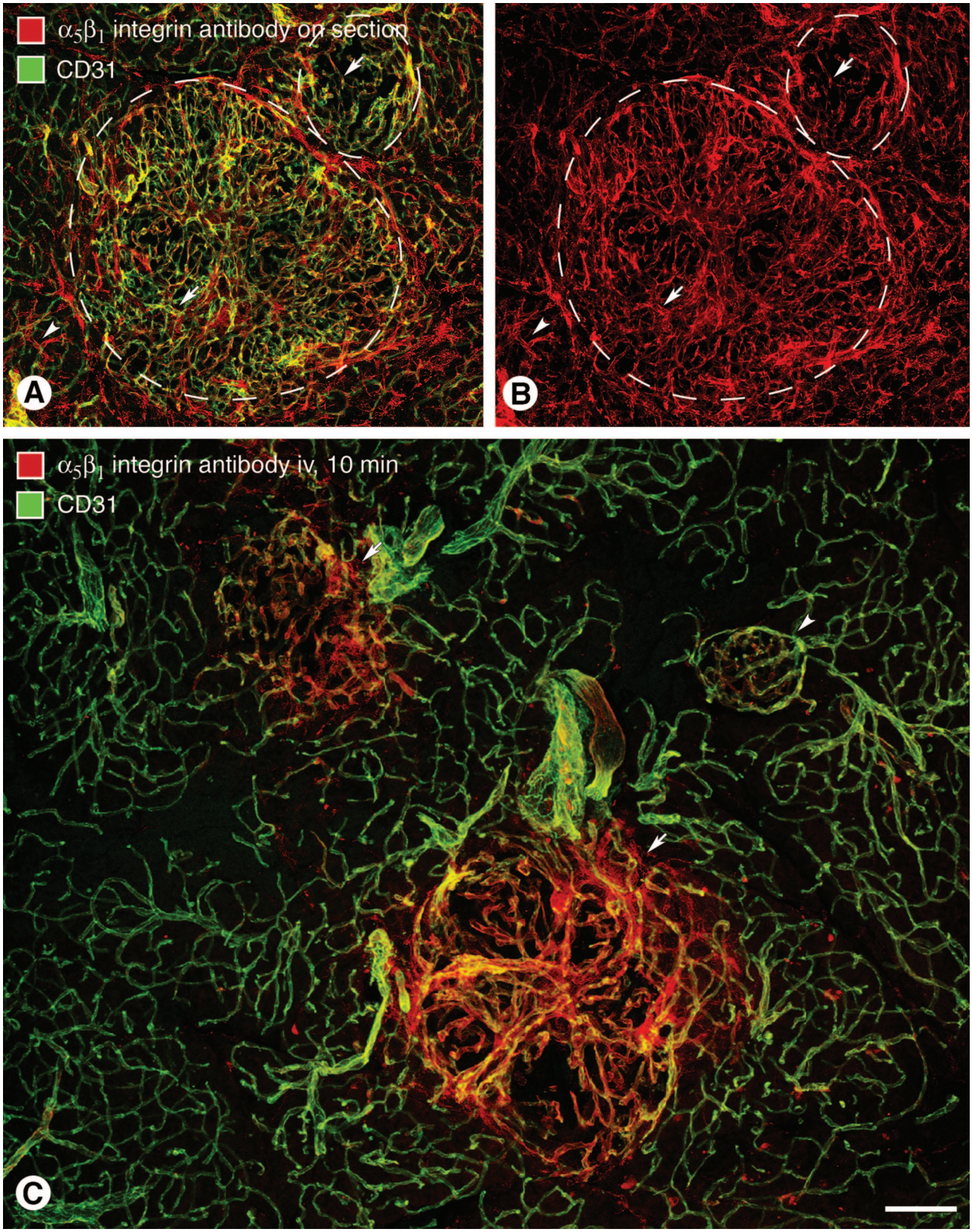

Figure 1. Rapidly accessible $\alpha_5\beta_1$ integrin on blood vessels of RIP-Tag2 tumors. Confocal microscopic images showing $\alpha_5\beta_1$ integrin immunoreactivity (red) and CD31 immunoreactivity (green) in pancreas of RIP-Tag2 mice. **A** and **B:** Blood vessels (**arrows**) in tumors (**outlined**) and pancreatic ducts (**arrowheads**) both have strong $\alpha_5\beta_1$ integrin immunoreactivity after staining by conventional immunohistochemistry. **A:** However, co-localization of CD31 (yellow-green) immunoreactivity co-localizes with $\alpha_5\beta_1$ integrin on tumor vessels but not on ducts (red) or normal blood vessels (green) of the acinar pancreas. **C:** At 10 minutes after intravenous injection of anti-$\alpha_5\beta_1$ integrin antibody, tumor vessels (**arrows**), but not pancreatic ducts or normal acinar vessels, have strong immunoreactivity. **C:** Normal-sized islet (**arrowhead**) in RIP-Tag2 mouse shows minimal binding of $\alpha_5\beta_1$ integrin antibody. Scale bar, 100 μm (**A**, **B**); 75 μm (**C**).

The extent of co-localization of anti-$\alpha_5\beta_1$ integrin and anti-CD31 antibodies in RIP-Tag2 tumors was calculated using the co-localization function of ImageJ (Figure 2).

Four images of one or more *apc* adenomas in each mouse were acquired by examining sequential sections of cross-sectioned intestinal rings. Four images of the MCa-IV carcinoma in each mouse were acquired by sampling at 3, 6, 9, and 12 o'clock around the circumference of the tumor. Each image of *apc* adenoma and MCa-IV carcinoma represented an ROI. Boundaries of *apc* adenomas and MCa-IV carcinomas were defined in separate images overexposed to highlight the tissue features.

A histogram displaying the number of pixels at fluorescence intensities 0 to 255 in each ROI was prepared using the histogram function of ImageJ (Figure 2). Data for each mouse included intensity histograms for ROI in three to four tumors of each size in RIP-Tag2 mice, four ROI per mouse for *apc* adenomas and MCa-IV carcinomas, or four ROI for normal tissues in wild-type mice. Histogram data were exported to Microsoft Excel, and mean values for the number of pixels at each intensity were calculated from multiple ROI to obtain a single intensity histogram for each tumor or tumor size for each mouse. Weighted values for fluorescence intensity were then calculated by multiplying the mean number of pixels at each intensity in the ROI by their corresponding brightness value of 0 to 255 (Figure 2). This transformation discarded all black values, because the intensity of black (background) pixels was evaluated as 0. The mean intensity for each mouse was then calculated as the sum of the weighted intensities for all brightness values divided by the total number of pixels in the ROI. Mean intensity values for all mice in a group were averaged to obtain an overall mean intensity for the group. Three-dimensional plots of fluorescence intensities of tissue sections, in which brightness was displayed in the *z* axis, were prepared with the Surface Plot function of ImageJ.

Tumor Vascularity

An index of vascular area density (proportion of sectional area occupied by tumor vessels) was measured in fluorescence microscopic digital images of specimens from RIP-Tag2 mice injected with $\alpha_5\beta_1$ integrin antibody to relate vascularity (number of labeled vessels per unit area) to the intensity of accumulated antibody (mean brightness per labeled site) in tumors of different size.[30] Area density measurements were made on three to four images of tumors of each of the three size groups per mouse ($\times$10 objective, $\times$1 Optovar, tissue region 960 $\times$ 1280 μm, $n = 4$ mice/group). Based on fluorescence intensities ranging from 0 to 255, specific vascular labeling by $\alpha_5\beta_1$ integrin antibody was distinguished from background by an empirically determined threshold value (intensity = 30) that included only blood vessels in specimens. Area density of vascular staining for $\alpha_5\beta_1$ integrin was calculated as the proportion of pixels having a fluorescence intensity equal to or greater than the corresponding threshold.[30] Tumors from RIP-Tag2 mice injected with IgG were handled in a similar manner as a control.

Statistics

The significance of differences among groups was tested by analysis of variance followed by Fisher's test for multiple comparisons or by Student's *t*-test using JMP v.5.0.1.2 (SAS Institute, Inc., Cary, NC). P values <0.05 were considered significant. All groups consisted of four mice, with the exception of *apc* mice injected with nonspecific IgG, which consisted of three mice. Results are presented as mean $\pm$ SE.

Results

Distribution and Accessibility of $\alpha_5\beta_1$ Integrin in RIP-Tag2 Tumors

Islet cell tumors and exocrine pancreas both had strong $\alpha_5\beta_1$ integrin immunoreactivity in RIP-Tag2 mouse tissues stained by conventional immunohistochemistry. Most of the staining in tumors was associated with blood vessels, but most staining in exocrine pancreas was associated with ducts (Figure 1, A and B). When anti-$\alpha_5\beta_1$ integrin antibody was injected intravenously, most of the immunoreactivity was associated with tumors, and little staining was evident in the exocrine pancreas (Figure 1C). Vessel immunoreactivity was stronger in tumors than in normal-size islets and increased in intensity with increasing tumor size (Figure 1C).

Measurement of Antibody Accumulation in Tumors

At 10 minutes after intravenous injection, $\alpha_5\beta_1$ integrin antibody labeled blood vessels in RIP-Tag2 tumors in a pattern that resembled the vascular network visible in tumor sections double-stained for CD31 by conventional on-section immunohistochemistry (Figure 2A). The amount of $\alpha_5\beta_1$ integrin antibody in tumors, assessed by analysis of the fluorescence intensity of pixels in digital images, was conspicuously greater than for nonspecific IgG (Figure 2B). The uniformity of $\alpha_5\beta_1$ integrin expression on tumor vessels was examined by comparing the distributions and amounts of anti-CD31 and anti-$\alpha_5\beta_1$ integrin antibodies on tumor vessels after simultaneous intravenous injection of both antibodies into RIP-Tag2 mice. At 10 minutes after injection, the two antibodies had similar distributions in tumors, as reflected by 85% co-localization of $\alpha_5\beta_1$ integrin pixels with CD31 pixels (Figure 2; C to F). In addition, area density measurements showed that the amounts of accumulation of CD31 and $\alpha_5\beta_1$ integrin antibodies were essentially the same (Figure 2G). However, the two antibodies did not have identical staining patterns outside of tumors. Anti-$\alpha_5\beta_1$ integrin antibody mainly labeled tumor vessels (Figure 2, C and D), but anti-CD31 stained the vasculature of the

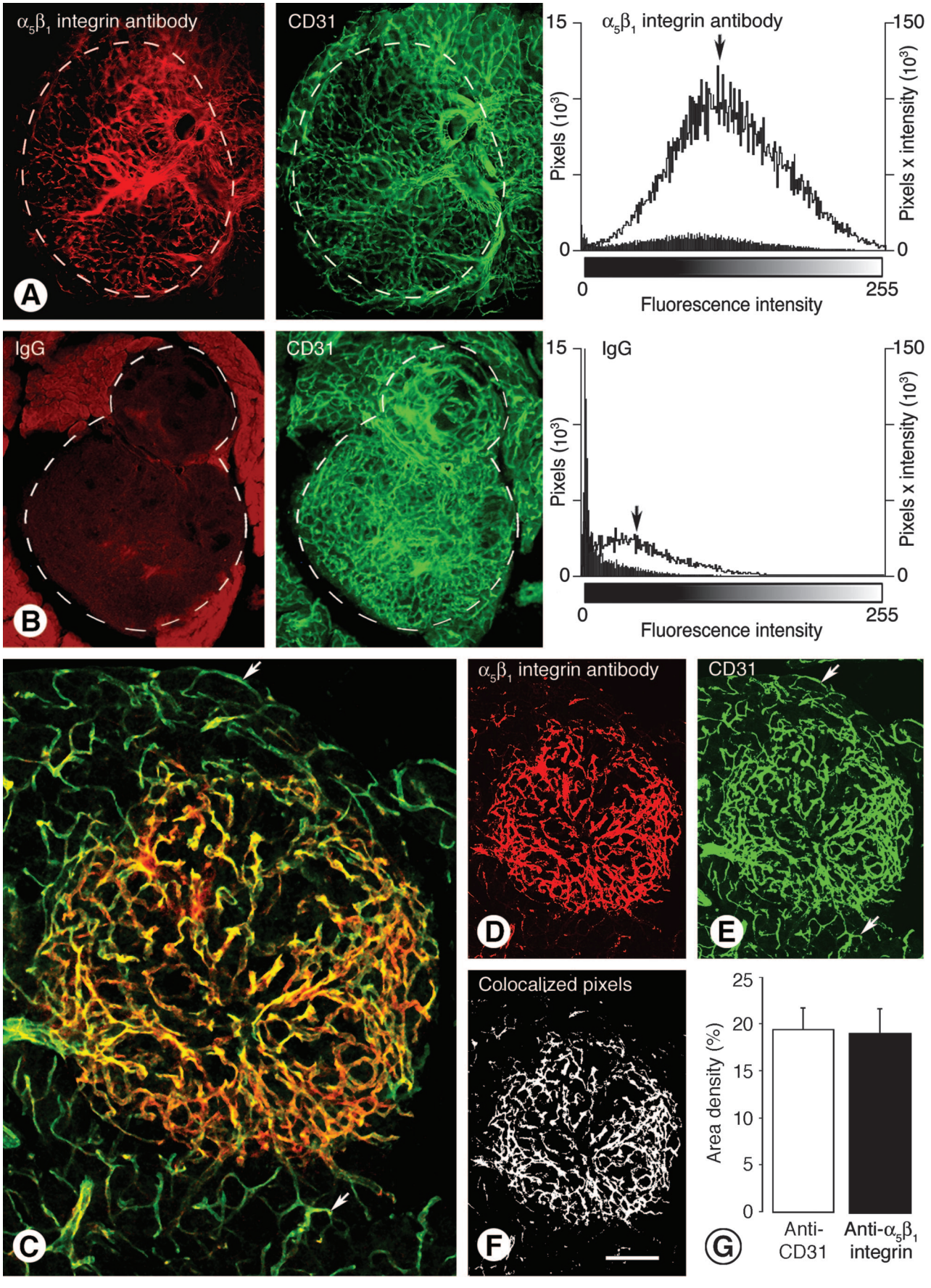
$\alpha_5\beta_1$ integrin antibody
CD31
A
15
150
$\alpha_5\beta_1$ integrin antibody
Pixels (10^3)
Pixels x intensity (10^3)
0
0
255
Fluorescence intensity
IgG
CD31
B
15
150
IgG
Pixels (10^3)
Pixels x intensity (10^3)
0
0
255
Fluorescence intensity
C
$\alpha_5\beta_1$ integrin antibody
D
CD31
E
Colocalized pixels
F
25
20
15
10
5
0
Area density (%)
Anti-CD31
Anti-$\alpha_5\beta_1$ integrin
G

acinar pancreas (Figure 2E) and other organs as well as tumor vessels.

Leakage of Antibodies in RIP-Tag2 Tumors

Labeling of tumor vessels by $\alpha_5\beta_1$ integrin antibody was accompanied by irregular patches of immunoreactivity around some vessels (Figure 3, A and B). These patches were outside blood vessels and appeared to be sites of antibody extravasation. Injection of nonspecific IgG resulted in similar extravascular patches, but the staining was weak and tumor vessels were not labeled (Figure 3, C and D). The differences in uniform vascular labeling by anti-$\alpha_5\beta_1$ integrin antibody and patchy leakage of IgG are illustrated schematically in Figure 3, E to G. The dense vascularity characteristic of RIP-Tag2 tumors is shown by on-section staining for CD31 (Figure 3E). Uniform binding of $\alpha_5\beta_1$ integrin antibody to tumor vessels has essentially the same pattern as CD31 immunoreactivity (Figure 3F). By comparison, sites of IgG leakage are located in patchy regions between tumor vessels (Figure 3G).

Kinetics of $\alpha_5\beta_1$ Integrin Distribution in RIP-Tag2 Tumors

Measurements of immunofluorescence in RIP-Tag2 tumors revealed significantly greater accumulation of anti-$\alpha_5\beta_1$ integrin antibody than nonspecific IgG at all time points from 10 minutes to 24 hours after intravenous injection (Figure 3H). Values for anti-integrin antibody were already high at 10 minutes, increased further through 6 hours, and then decreased to the 10-minute level at 24 hours (Figure 3H). Extravasated nonspecific IgG was barely detectable at 10 minutes, increased a bit at 1 hour, but remained less than half the value for anti-integrin antibody throughout the 24-hour period of the study (Figure 3H).

Distribution and Accessibility of $\alpha_5\beta_1$ Integrin in Normal Islets

The vasculature of normal islets in wild-type pancreas had weak $\alpha_5\beta_1$ integrin immunoreactivity when stained by conventional immunohistochemistry (Figure 4, A and B). Ducts of normal acini had stronger staining (Figure 4B). Yet, when the antibody was injected intravenously, islet vasculature stained weakly, but ducts had little or no immunoreactivity (Figure 4, C and D). Pancreatic islets and ducts had little or no immunoreactivity after injection of nonspecific IgG (Figure 4, E and F).

Increased $\alpha_5\beta_1$ Integrin Expression during Progression of RIP-Tag2 Tumors

Expression of $\alpha_5\beta_1$ integrin increased with tumor size in RIP-Tag2 mice. More circulating anti-$\alpha_5\beta_1$ integrin antibody accumulated in small tumors than in normal islets of wild-type mice (Figure 5; A to F). There was even greater accumulation of antibody in large tumors, which was evident in images and in surface plots of immunofluorescence (Figure 5, G and H). Measurements of fluorescence intensity showed the magnitude of these size-related differences and the differences between the accumulation of anti-$\alpha_5\beta_1$ integrin antibody and nonspecific IgG after intravenous injection (Figure 5I). The mean intensity of $\alpha_5\beta_1$ integrin immunofluorescence in RIP-Tag2 tumors was three times the value for normal islets in wild-type mice and for nonspecific IgG in tumors.

Increasing vascularity with tumor enlargement, as shown by increases in area density of $\alpha_5\beta_1$ integrin labeling (Figure 5J), contributed to the increased accumulation of circulating $\alpha_5\beta_1$ integrin antibody. However, comparison of surface plots of tissue fluorescence for anti-$\alpha_5\beta_1$ integrin antibody in tumors of different size (Figure 5; C, F, and H) demonstrated that intensity of labeling (height of peaks = antibody binding per vessel) increased even more than the number of labeled sites (number of peaks = vascularity).

Distribution and Accessibility of $\alpha_5\beta_1$ Integrin in apc *Intestinal Adenomas*

Intestinal adenomas of *apc* mice had strong $\alpha_5\beta_1$ integrin immunoreactivity when stained by conventional immunohistochemistry (Figure 6A). The greatest staining was associated with blood vessels, stromal cells, and some tumor cells of the adenomas. Strong $\alpha_5\beta_1$ integrin immunoreactivity was also present in smooth muscle cells of the intestinal wall (Figure 6A) and intestinal villi (Figure 6B),[34] both in *apc* mice and in wild-type mice. The identity of smooth muscle cells was confirmed by co-localization with α-smooth muscle actin immunoreactivity (data not shown). Immunoreactivity for $\alpha_5\beta_1$ integrin was not detected in the micro-

Figure 2. Amount and distribution of antibodies in tumors. Pairs of fluorescence microscopic images of RIP-Tag2 tumors fixed 10 minutes after intravenous injection of anti-$\alpha_5\beta_1$ integrin antibody (**A**, **left**) or nonspecific IgG (**B**, **left**). Both sections are also stained for CD31 immunoreactivity (**right**). **Dashed lines** mark tumor perimeter and define the ROI used for fluorescence measurements. In graphs of **A** and **B**, lower histogram (**solid**) shows number of pixels at fluorescence intensities ranging from 0 (black) to 255 (white) in the ROI of a grayscale version of the corresponding red-fluorescent image (*y* axis, **left**). Upper histogram (**open**) of each graph shows distribution of weighted intensities calculated by multiplying pixel frequencies by their respective fluorescence intensities (*y* axis, **right**). **Arrows** mark arithmetic means of weighted intensities. **C:** Confocal micrograph of tumor in RIP-Tag2 mouse at 10 minutes after intravenous injection of anti-CD31 (green) and anti-$\alpha_5\beta_1$ integrin antibodies (red). Most blood vessels within the central round tumor are labeled by both antibodies (yellow-orange), but those in the surrounding acinar pancreas are labeled only by the anti-CD31 antibody (**arrows**). **D–F:** Binary images of **C** that show the distribution of anti-$\alpha_5\beta_1$ integrin (**D**), anti-CD31 (**E**) pixels above a threshold intensity of 60, and the pixels where the two antibodies co-localize (**F**, white). **Arrows** in **E** mark vessels in acinar pancreas. In this case, 85% of $\alpha_5\beta_1$ integrin pixels co-localize with CD31 pixels. **G:** Bar graph showing the area densities of anti-CD31 and anti-$\alpha_5\beta_1$ integrin antibodies in RIP-Tag2 tumors 10 minutes after injection (20 images of 20-μm sections of tumors from three mice, threshold = 35). Scale bar, 100 μm (**A**, **B**, **D–F**); 50 μm (**C**).

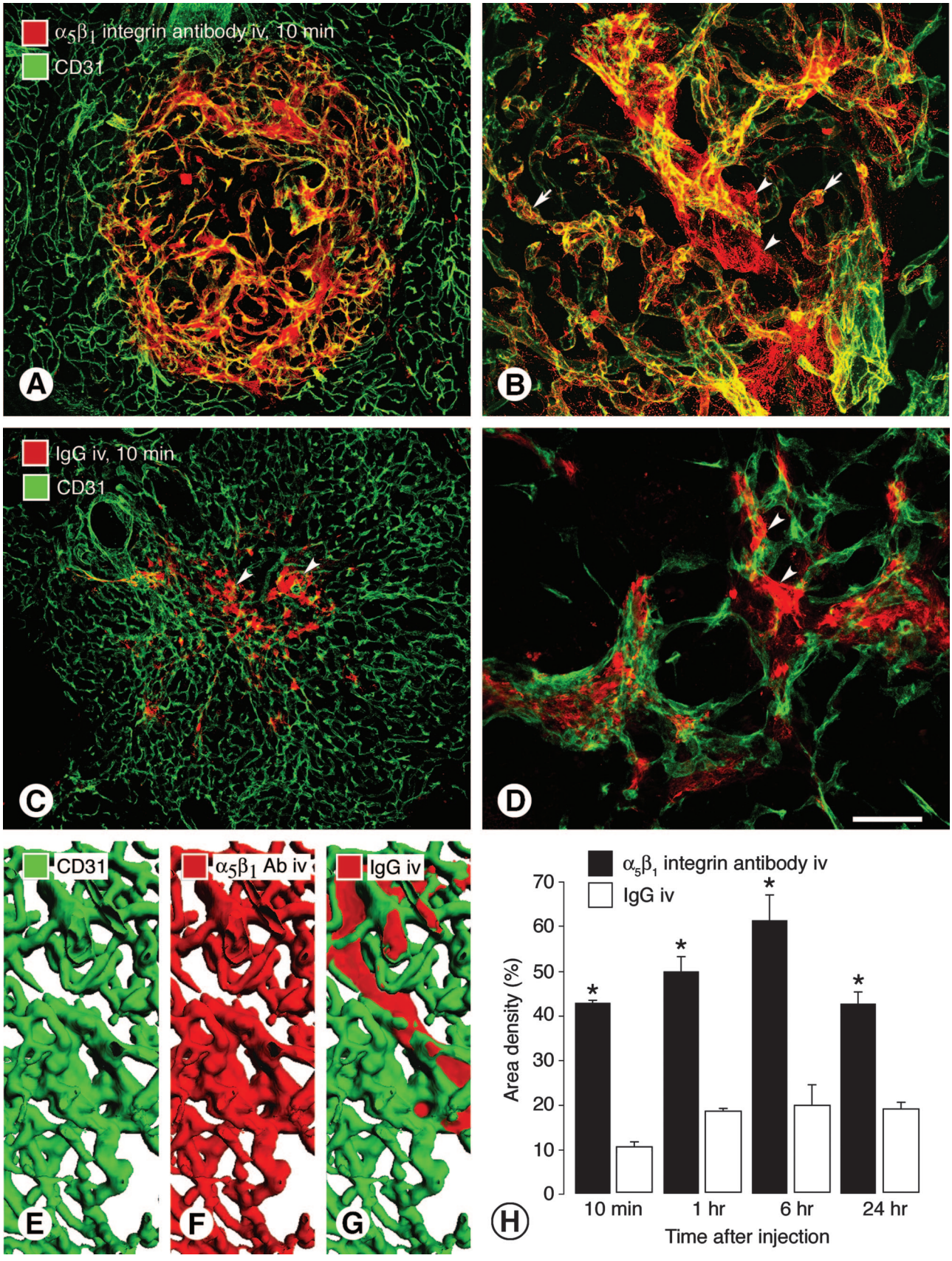
α5β1 integrin antibody iv, 10 min
CD31
A
B
IgG iv, 10 min
CD31
C
D
CD31
α5β1 Ab iv
IgG iv
E
F
G
α5β1 integrin antibody iv
IgG iv
Area density (%)
70
60
50
40
30
20
10
0
*
*
*
*
10 min
1 hr
6 hr
24 hr
Time after injection
H

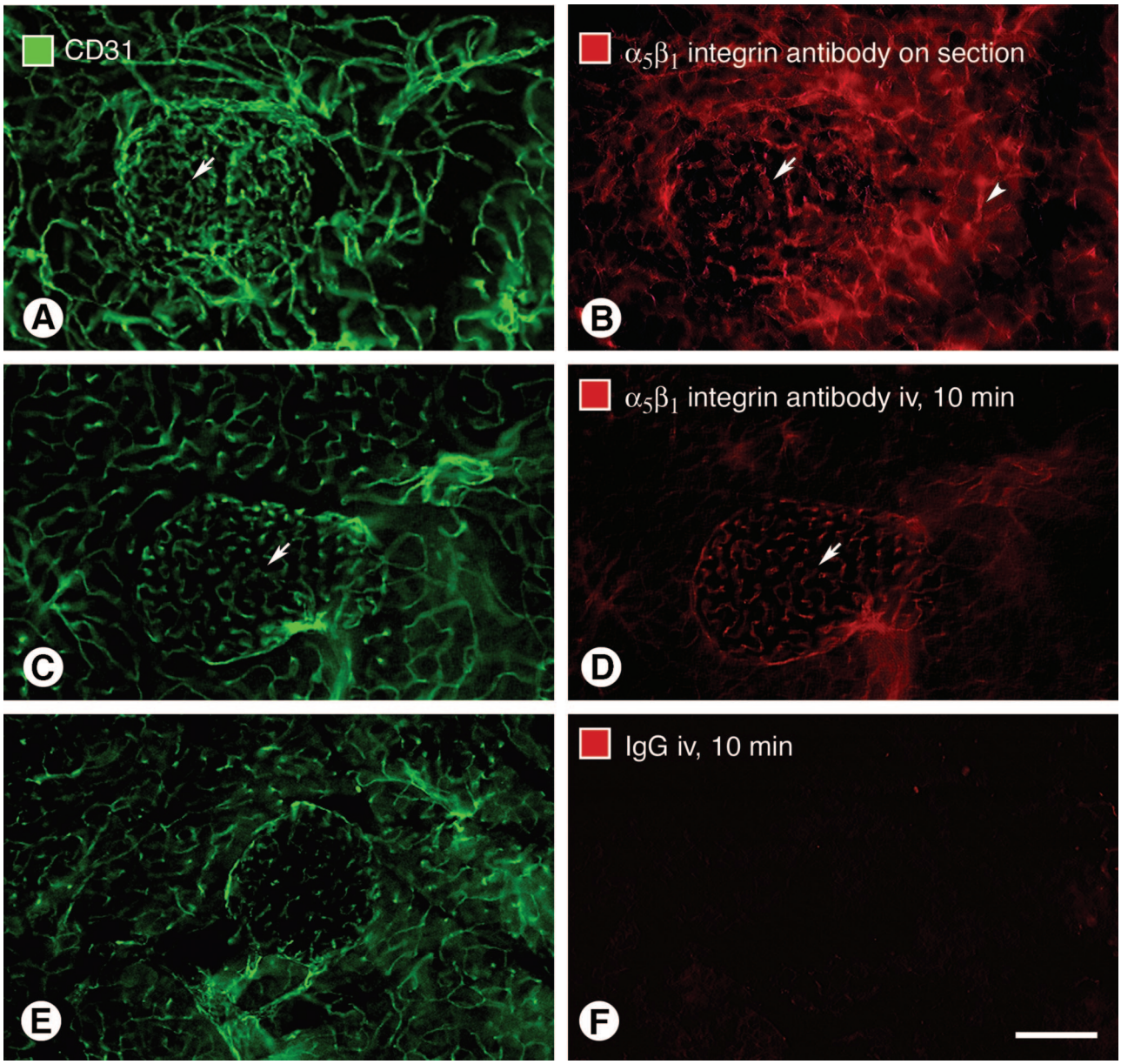

Figure 4. Weak $\alpha_5\beta_1$ integrin immunoreactivity of normal islet blood vessels. Confocal microscopic images showing immunoreactivity of CD31 (green) and $\alpha_5\beta_1$ integrin (red) in normal pancreatic islets. When stained for $\alpha_5\beta_1$ integrin by conventional immunohistochemistry, blood vessels of islets have weak immunoreactivity (**A** and **B**, **arrow**), and ducts of pancreatic acini have strong immunoreactivity (**B**, **arrowhead**). **C** and **D:** After injection of anti-$\alpha_5\beta_1$ integrin antibody, islet blood vessels have weak immunoreactivity (**arrow**) and ducts have little or none. **E** and **F:** After injection of nonspecific IgG, normal islets and acini have little or no staining for IgG. Scale bar, 50 μm.

vasculature or epithelium of normal intestinal villi in wild-type or *apc* mice (Figure 6B).

The pattern of staining in the intestine was very different after intravenous injection of anti-$\alpha_5\beta_1$ integrin antibody. Blood vessels and smooth muscle cells had little or no $\alpha_5\beta_1$ integrin immunoreactivity in normal intestinal villi (Figure 6C), but blood vessels of *apc* adenomas had intense immunoreactivity (Figure 6, D and E). Vascular staining in adenomas had indistinct borders suggestive of antibody extravasation and binding to stromal cells (Figure 6, D and

Figure 3. Rapid accumulation of anti-$\alpha_5\beta_1$ integrin antibody versus patchy leakage of nonspecific IgG in RIP-Tag2 tumors. **A–D:** Confocal microscopic images showing distribution of intravenously injected anti-$\alpha_5\beta_1$ integrin antibody or nonspecific IgG (red) in relation to CD31-positive blood vessels (green) in RIP-Tag2 tumors. **A:** Most immunoreactivity of anti-$\alpha_5\beta_1$ integrin antibody co-localizes with CD31 staining of blood vessels within the tumor (yellow-orange) but not with normal vessels (green) outside the tumor. **B:** At higher magnification, anti-$\alpha_5\beta_1$ integrin antibody can be seen to label blood vessels (yellow-orange, **arrows**) and accumulate in scattered patches of extravasation (red, **arrowheads**) in tumors. **C** and **D:** By comparison, immunoreactivity for nonspecific IgG is patchy, does not co-localize with CD31-positive tumor vessels, and is primarily extravascular. **E–G:** Schematic representation comparing the uniform labeling of RIP-Tag2 tumor vessels by anti-CD31 (**E**, green) and anti-$\alpha_5\beta_1$ integrin (**F**, red) antibodies with the patchy extravasation of nonspecific IgG (**G**, red) without vessel labeling. **H:** Bar graph showing the kinetics of accumulation of injected anti-$\alpha_5\beta_1$ integrin antibody and nonspecific IgG in RIP-Tag2 tumors. Anti-integrin antibody accumulated faster and in greater amounts than IgG at all time points ($^*P < 0.05$). Scale bar, 100 μm (**A**, **C**); 50 μm (**B**, **D**).

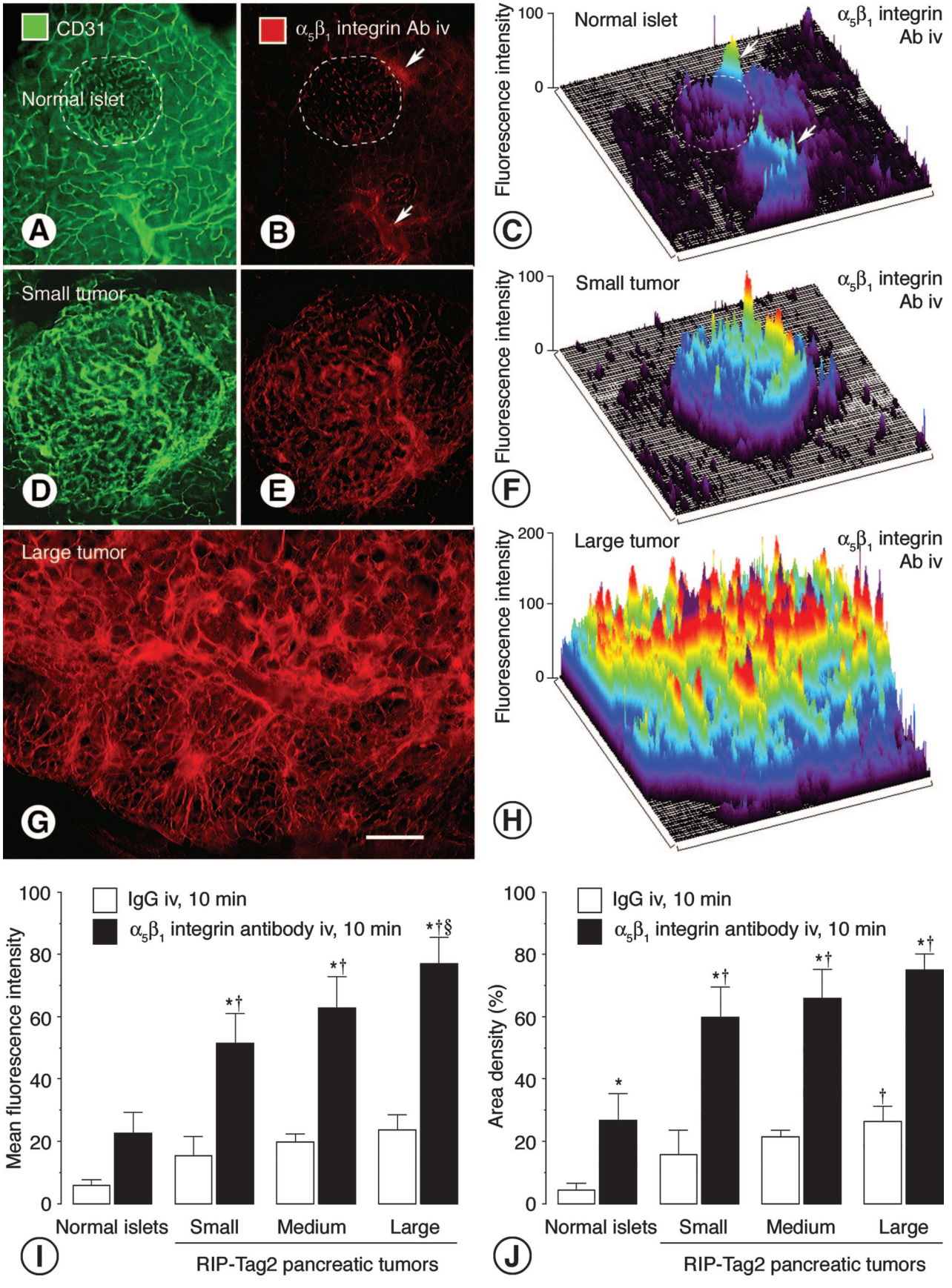
CD31
Normal islet
A
$\alpha_5\beta_1$ integrin Ab iv
B
Small tumor
D
E
Large tumor
G
Normal islet
$\alpha_5\beta_1$ integrin Ab iv
Fluorescence intensity
100
0
C
Small tumor
$\alpha_5\beta_1$ integrin Ab iv
Fluorescence intensity
100
0
F
Large tumor
$\alpha_5\beta_1$ integrin Ab iv
Fluorescence intensity
200
100
0
H
IgG iv, 10 min
$\alpha_5\beta_1$ integrin antibody iv, 10 min
Mean fluorescence intensity
100
80
60
40
20
0
*†
*†
*†§
Normal islets
Small
Medium
Large
RIP-Tag2 pancreatic tumors
I
IgG iv, 10 min
$\alpha_5\beta_1$ integrin antibody iv, 10 min
Area density (%)
100
80
60
40
20
0
*
*†
*†
*†
†
Normal islets
Small
Medium
Large
RIP-Tag2 pancreatic tumors
J

E). This stromal staining had a patchy distribution and was greatest near the apical surface of adenomas (Figure 6F). After intravenous injection of nonspecific IgG, patches of faint, diffuse immunoreactivity were scattered in adenomas of *apc* mice (Figure 6G). Measurements of immunofluorescence in *apc* adenomas showed that the mean value for anti-$\alpha_5\beta_1$ integrin antibody after intravenous injection was twice the corresponding value for normal intestine and fourfold the value for *apc* adenomas after injection of nonspecific IgG (Figure 7).

Distribution and Accessibility of $\alpha_5\beta_1$ Integrin in MCa-IV Mammary Carcinomas

Blood vessels and scattered tumor cells had strong $\alpha_5\beta_1$ integrin immunoreactivity in implanted MCa-IV carcinomas stained by conventional immunohistochemistry (data not shown). Strong immunoreactivity was also present in these tumors after intravenous injection of the antibody, but here most of the staining was associated with blood vessels (Figure 8, A and B). Little or no staining was found after injection of nonspecific IgG (Figure 8, C and D). Fluorescence measurements showed that immunoreactivity of MCa-IV carcinomas was 7.5-fold greater after intravenous injection of anti-$\alpha_5\beta_1$ integrin antibody than after injection of nonspecific IgG (Figure 7).

Distribution and Accessibility of $\alpha_5\beta_1$ Integrin in Normal Organs

To develop a perspective for interpreting the rapid, uniform labeling of tumor vessels by intravascular anti-$\alpha_5\beta_1$ integrin antibody, immunohistochemically stained sections of several normal organs and tumors prepared 10 minutes after injection of anti-$\alpha_5\beta_1$ integrin antibody or nonspecific IgG were imaged at standardized camera settings optimized for the Cy3 (yellow-orange) fluorophore (Figure 9, Table 1). The microvasculature of most normal organs had little or no detectable anti-$\alpha_5\beta_1$ integrin antibody immunoreactivity (Table 1). Brain (Figure 9, A and B), lung, and testis were examples of organs with negligible staining. The absence of staining in these organs appeared to result from absence of $\alpha_5\beta_1$ integrin rather than absence of antibody leakage, because no immunoreactivity was found in brain vasculature stained for $\alpha_5\beta_1$ integrin by conventional immunohistochemistry, except for faint staining of large cerebral arteries (data not shown).

Sinusoids of the liver were notable exceptions. Hepatic sinusoids had strong immunoreactivity after intravenous injection of anti-$\alpha_5\beta_1$ integrin antibody (Figure 9C, left; Table 1). Liver of tumor-bearing mice and normal mice was similar in this regard. This staining was not the result of antibody accumulation around highly permeable hepatic sinusoids because strong $\alpha_5\beta_1$ integrin immunoreactivity was also found in liver stained for the integrin by conventional immunohistochemistry (Figure 9C, right). Also, intravenous injection of nonspecific IgG, which would also leak, produced only faint staining (Figure 9D). Although the overall staining of hepatic sinusoids after injection of anti-$\alpha_5\beta_1$ integrin antibody was even more intense than was found in the vessels of RIP-Tag2 tumors (Figure 9E), the higher vascular density of the liver limited the meaningfulness of this comparison. Faint staining of the liver after intravenous injection of nonspecific IgG was approximately the same as found in RIP-Tag2 tumors under the same conditions (Figure 9F, Table 1). High endothelial venules of lymph nodes were another site where strong immunoreactivity was present after injection of anti-$\alpha_5\beta_1$ integrin antibody (Figure 9G, Table 1). These vessels had little or no staining after injection of nonspecific IgG (Figure 9H).

Assessment of Potential Toxicity of Injected Anti-$\alpha_5\beta_1$ Integrin Antibody

No adverse effects of anti-$\alpha_5\beta_1$ integrin antibody were detected in RIP-Tag2 mice during the 10-minute to 24-hour period of circulation in the bloodstream. None of the mice died or show signs of distress. Histological studies on tissues from these mice revealed no evidence of pathological changes in any of 11 organs, including the liver where sinusoidal endothelial cells were strongly labeled by the antibody.

Discussion

The goal of this study was to compare the overall cellular distribution of $\alpha_5\beta_1$ integrin in normal organs and tumors and to identify sites where the integrin was highly expressed and readily accessible to intravascular antibodies. We found that most normal blood vessels in mice had little or no $\alpha_5\beta_1$ integrin immunoreactivity. Although pancreatic ducts, intestinal smooth muscle, and some other normal tissues did have strong staining by conventional immunohistochemistry, this was not the case when the same antibody was injected into the bloodstream, indicating that anti-$\alpha_5\beta_1$ integrin antibody had limited access to these sites during the 10-minute period of circulation.

Figure 5. Increasing binding of intravenously injected anti-$\alpha_5\beta_1$ integrin antibody during tumor progression. Fluorescence micrographs and corresponding surface plots of tissue fluorescence showing islet in wild-type mouse (**A–C**, **dashed circle**) and small tumor (**D–F**) and large tumor (**G–H**) in RIP-Tag2 mice. CD31 stained on-section by conventional immunohistochemistry (green). Immunoreactivity of anti-$\alpha_5\beta_1$ integrin antibody at 10 minutes after intravenous injection (red). Height of peaks in surface plots indicates intensity of immunofluorescence. Number of peaks reflects vascularity. **I:** Bar graph showing intensity of antibody fluorescence at 10 minutes after intravenous injection of anti-$\alpha_5\beta_1$ integrin antibody or nonspecific IgG in RIP-Tag2 mice. After intravenous injection of anti-$\alpha_5\beta_1$ integrin antibody, the immunoreactivity is greater in RIP-Tag2 tumors than in normal islets. This difference increases during tumor progression, as reflected by increasing tumor size. Fluorescence of extravasated nonspecific IgG tends to increase with increasing tumor size, presumably reflecting increased extravasation during tumor progression. However, fluorescence from nonspecific IgG is consistently less than corresponding values for anti-$\alpha_5\beta_1$ integrin antibody. **J:** Area densities of nonspecific IgG and anti-$\alpha_5\beta_1$ integrin antibody immunofluorescence in the same tumors as **I** reflect tumor vascularity. Vascularity is significantly greater in tumors than in normal islets, but the values are about the same for tumors of different size. Mean ± SE; $n = 4$ mice per group. $^{*}P < 0.05$ for anti-$\alpha_5\beta_1$ integrin antibody compared to nonspecific IgG; $^{\dagger}P < 0.05$ for tumors compared to normal islets; $^{\S}P < 0.05$ for large tumors compared to small tumors. Scale bar,150 μm.

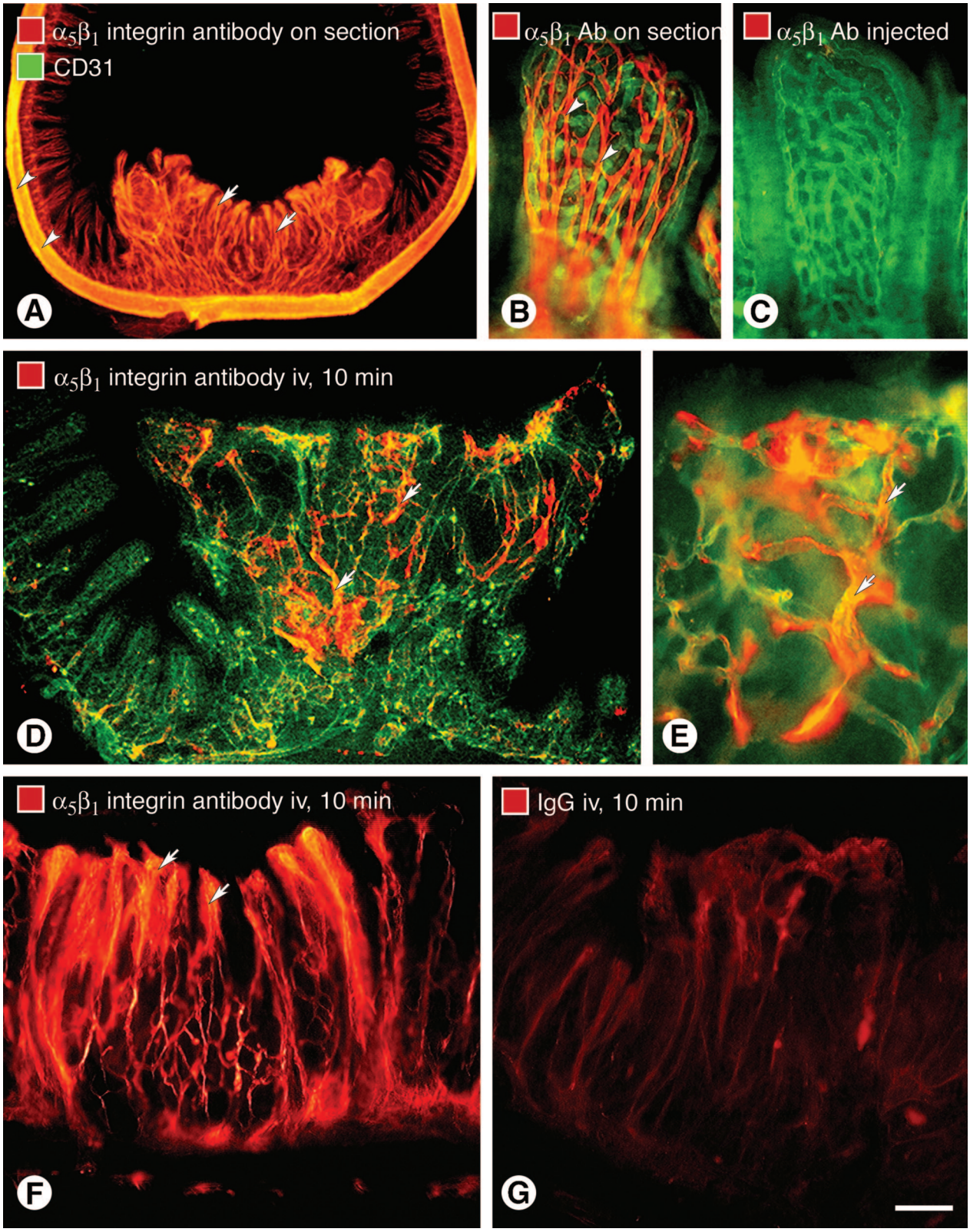

Figure 6. Rapidly accessible $\alpha_5\beta_1$ integrin on blood vessels of intestinal adenomas in *apc* mice. Fluorescence microscopic images showing $\alpha_5\beta_1$ integrin immunoreactivity (red) and CD31 immunoreactivity of blood vessels (green) in adenomas and normal intestine of *apc* mice. **A:** Strong $\alpha_5\beta_1$ integrin immunoreactivity is evident in intestinal adenoma (**arrows**) and smooth muscle of the intestinal wall (**arrowheads**) after conventional on-section immunohistochemical staining. **B:** Smooth muscle cells (**arrowheads**) of normal intestinal villi also have strong immunoreactivity. At 10 minutes after intravenous injection of anti-$\alpha_5\beta_1$ integrin antibody, neither smooth muscle cells nor blood vessels of normal intestinal villi have immunoreactivity (**C**), but blood vessels (**arrow**) in adenomas have strong staining (**D**). **E:** Blood vessel staining in adenomas has fuzzy borders suggestive of antibody leakage and binding to perivascular cells. **F:** Diffuse staining (**arrows**) is greatest in the apical portion of adenomas. **G:** By comparison, adenomas have much fainter and more patchy staining after injection of nonspecific IgG, consistent with labeling of extravasated IgG rather than blood vessels. Scale bar, 200 μm (**A**); 10 μm (**B**, **C**, **E**); 150 μm (**D**); 100 μm (**F**, **G**).

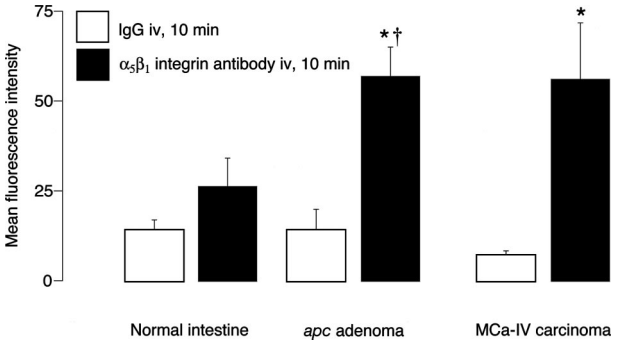

Figure 7. Immunofluorescence of intravenously injected anti-$\alpha_5\beta_1$ integrin antibody in *apc* adenomas and MCa-IV carcinomas. Bar graph comparing immunofluorescence intensity at 10 minutes after intravenous injection of anti-$\alpha_5\beta_1$ integrin antibody or nonspecific IgG in normal intestine, intestinal adenomas in *apc* mice, and implanted MCa-IV mammary carcinomas. After intravenous injection of anti-$\alpha_5\beta_1$ integrin antibody, antibody fluorescence is greater in *apc* tumors than in normal intestine. Both *apc* adenomas and MCa-IV carcinomas have significantly greater staining for anti-$\alpha_5\beta_1$ integrin antibody than for nonspecific IgG. Mean ± SE; $n = 4$ mice per group ($n = 3$ for nonspecific IgG in *apc* adenomas). $^*P < 0.05$ compared to nonspecific IgG; $^\dagger P < 0.05$ compared to corresponding value for normal intestine.

By comparison, $\alpha_5\beta_1$ integrin on blood vessels in three murine tumor models—islet cell tumors in RIP-Tag2 transgenic mice, intestinal adenomas in *apc* mice, and MCa-IV mammary carcinomas—was uniformly overexpressed and was rapidly accessible to intravascular antibody. Immunofluorescence measurements showed that most of the accumulation of anti-$\alpha_5\beta_1$ integrin antibody in tumors resulted from direct labeling of tumor vessels rather than vessel leakiness. Overall accumulation of antibody in tumors, as reflected by immunofluorescence at 10 minutes to 24 hours after injection, was two to seven times the accumulation of extravasated nonspecific IgG. These findings indicate that $\alpha_5\beta_1$ integrin is overexpressed on tumor blood vessels and rapidly accessible to antibodies in the bloodstream.

Role of $\alpha_5\beta_1$ Integrin in Angiogenesis

The integrin $\alpha_5\beta_1$ and its principal ligand fibronectin are essential for normal embryonic development. Targeted deletion of either the α_5 integrin subunit or fibronectin results in major disturbances in the vasculature and embryonic lethality.[35–37] Mouse embryos lacking α_5 integrin have distended blood vessels and abnormal vascular patterning.[37]

In the adult, $\alpha_5\beta_1$ integrin promotes angiogenesis and is essential for the growth of new blood vessels under some conditions.[14] Both $\alpha_5\beta_1$ integrin and fibronectin are up-regulated in angiogenesis in tumors[13,24] and certain other diseases.[38] Integrin $\alpha_5\beta_1$ on blood vessels is up-regulated by basic fibroblast growth factor (bFGF, FGF2), tumor necrosis factor-α, or interleukin-8 but not by vascular endothelial growth factor (VEGF).[13] Expression of $\alpha_5\beta_1$ integrin is regulated by the homeobox transcription factor Hox D3, which induces expression by binding directly to the promoter of the integrin α_5 subunit.[39]

Integrin $\alpha_5\beta_1$ promotes angiogenesis by supporting endothelial cell migration and survival.[14,40] This process is mediated in part by suppression of an apoptotic program dependent on protein kinase A activity.[14] Integrin $\alpha_5\beta_1$ may also play a role in angiogenesis by serving as a binding site for fibrinogen[41,42] and endostatin.[43] Inhibition of $\alpha_5\beta_1$ integrin signaling may lead to caspase-3- and caspase-8-dependent endothelial cell death via apoptosis.[13,14] This mechanism has been exploited in preclinical models in which tumor growth has been slowed by inhibition of $\alpha_5\beta_1$ integrin.[13,14,24] In this regard, $\alpha_5\beta_1$ integrin, like $\alpha_v\beta_3$ integrin, is a potential target for inhibiting angiogenesis.[12,44–46]

Tissue Distribution $\alpha_5\beta_1$ Integrin

The present study showed that $\alpha_5\beta_1$ integrin is highly expressed by a variety of normal cell types of mice, including epithelial cells of pancreatic ducts and smooth muscle cells of the intestinal wall and villi, which are also sites of expression in humans.[47,48] However, most normal blood vessels in adult mice had little or no expression of $\alpha_5\beta_1$ integrin detectable by conventional immunohistochemistry. Two exceptions were hepatic sinusoids and high-endothelial venules of lymph nodes. Unlike $\alpha_5\beta_1$ integrin, fibronectin is nearly ubiquitous in basement membranes of normal adult tissues.[49]

In contrast to their normal counterparts, blood vessels in RIP-Tag2 tumors, *apc* adenomas, and MCa-IV carcinomas had uniformly strong expression of $\alpha_5\beta_1$ integrin. The finding of strong immunoreactivity of blood vessels in these tumors is consistent with the documented increased expression of $\alpha_5\beta_1$ integrin on tumor vessels.[13,24,30,50,51] In RIP-Tag2 tumors and MCa-IV carcinomas, most $\alpha_5\beta_1$ integrin expression was associated with vascular endothelial cells, whereas in *apc* adenomas, the integrin was expressed not only by blood vessels but also by stromal cells and to a lesser extent tumors cells.

Increasing $\alpha_5\beta_1$ Integrin Expression during Tumor Progression

The use of the RIP-Tag2 model made it possible to follow changes in $\alpha_5\beta_1$ integrin expression during tumor progression. The changes were assessed by comparing the accumulation of anti-$\alpha_5\beta_1$ integrin antibody. Faint immunoreactivity was detected on blood vessels of normal pancreatic islets, but labeling was significantly greater in blood vessels of even the smallest tumors, and the amount of anti-$\alpha_5\beta_1$ integrin antibody that accumulated increased with tumor size. The change in antibody binding appeared to result both from increased expression of the integrin on tumor vessels and from increased tumor vascularity. Fluorescence measurements and surface plots of immunofluorescence showed increases in both the height of the fluorescence intensity peaks, reflecting amount of antibody binding per vessel, as well as the number of peaks, reflecting the density of the vasculature.[30]

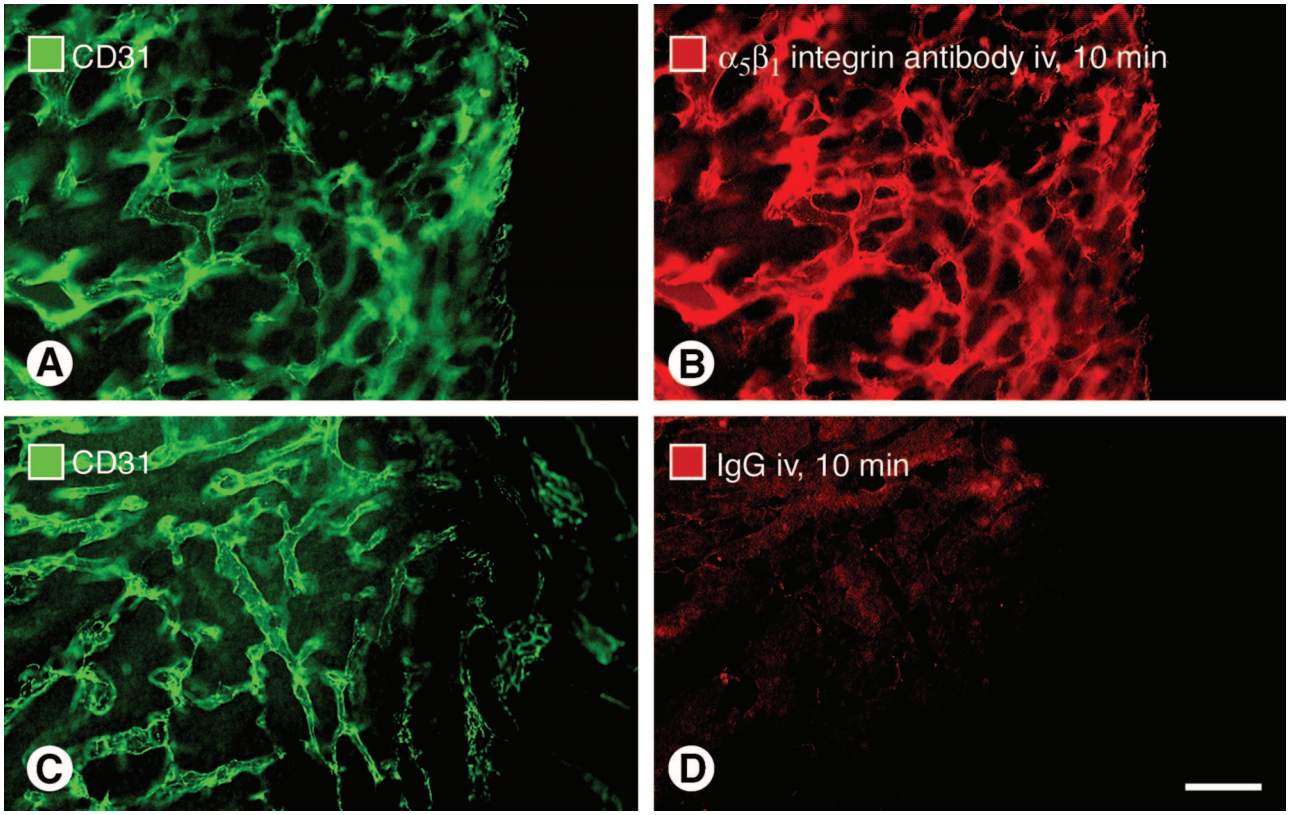

Figure 8. Rapidly accessible $\alpha_5\beta_1$ integrin on blood vessels of MCa-IV mammary carcinomas. Fluorescence micrographs showing CD31-positive blood vessels (**A**, **C**; green) and comparing immunoreactivity (red) for injected anti-$\alpha_5\beta_1$ integrin antibody or nonspecific IgG in MCa-IV mammary carcinomas. At 10 minutes after intravenous injection of anti-$\alpha_5\beta_1$ integrin antibody, tumor vessels have uniform staining (**B**), but after injection of nonspecific IgG, staining is faint and patchy, and does not co-localize with tumor vessels (**D**). Scale bar, 100 μm.

Accessibility of $\alpha_5\beta_1$ Integrin

One objective of the present study was to test the accessibility of sites of $\alpha_5\beta_1$ integrin expression in tumors to antibodies in the bloodstream. To address this issue we injected anti-$\alpha_5\beta_1$ integrin antibody into the circulation and then compared the amount and distribution of labeling at 10 minutes with that found by conventional immunohistochemistry. The brief circulation time was part of the experimental design to identify sites of greatest accessibility to the antibody. At 10 minutes, labeling was restricted to tumor vessels and scattered focal sites of leakage nearby.

Intravascular anti-$\alpha_5\beta_1$ integrin antibody prominently labeled blood vessels in all three tumor models. In RIP-Tag2 mice, preferential labeling of tumor vessels sharply highlighted pancreatic tumors against the remainder of the pancreas. Strikingly different results were obtained when the antibody was injected versus when it was applied directly to tissue sections. Conventional immunohistochemistry showed that $\alpha_5\beta_1$ integrin was expressed by multiple cell types both in tumors and in some normal organs.

Kinetic studies of anti-$\alpha_5\beta_1$ integrin antibody injected into RIP-Tag2 mice revealed that the labeling of tumor vessels was already strong at 10 minutes. Thereafter, the amount of labeling increased somewhat throughout 6 hours and remained high for the entire 24-hour period of the study. The amount of labeling by the anti-integrin antibody significantly exceeded that produced by extravasated nonspecific IgG at all time points. Accumulation of nonspecific IgG in tumors and of antibodies was manifested by patches of leakage rather than vascular labeling. No intravascular IgG remained after the blood was removed by vascular perfusion of fixative.

Co-localization of $\alpha_5\beta_1$ integrin with sites of CD31 immunoreactivity confirmed that endothelial cells were the main cellular location of rapidly accessible integrin in tumors. Injection of anti-$\alpha_5\beta_1$ integrin and anti-CD31 antibodies together gave very similar results in tumors, where both antibodies labeled most tumor vessels and most $\alpha_5\beta_1$ integrin co-localized with CD31. However, the two antibodies gave very different results elsewhere because of the generalized vascular labeling by the CD31 antibody.

It was not surprising that anti-CD31 antibody rapidly labeled tumor vessels, but why were tumor vessels preferentially labeled by intravascular anti-$\alpha_5\beta_1$ integrin antibody? Access of antibodies in the bloodstream to $\alpha_5\beta_1$ integrin in tumors is determined by the anatomical distribution of sites of integrin expression, macromolecular permeability of the vasculature at those sites, convective driving forces, and endothelial surface area for antibody extravasation.[19] The well documented leakiness of blood vessels in tumors may be a factor.[52] Indeed, the vascu-

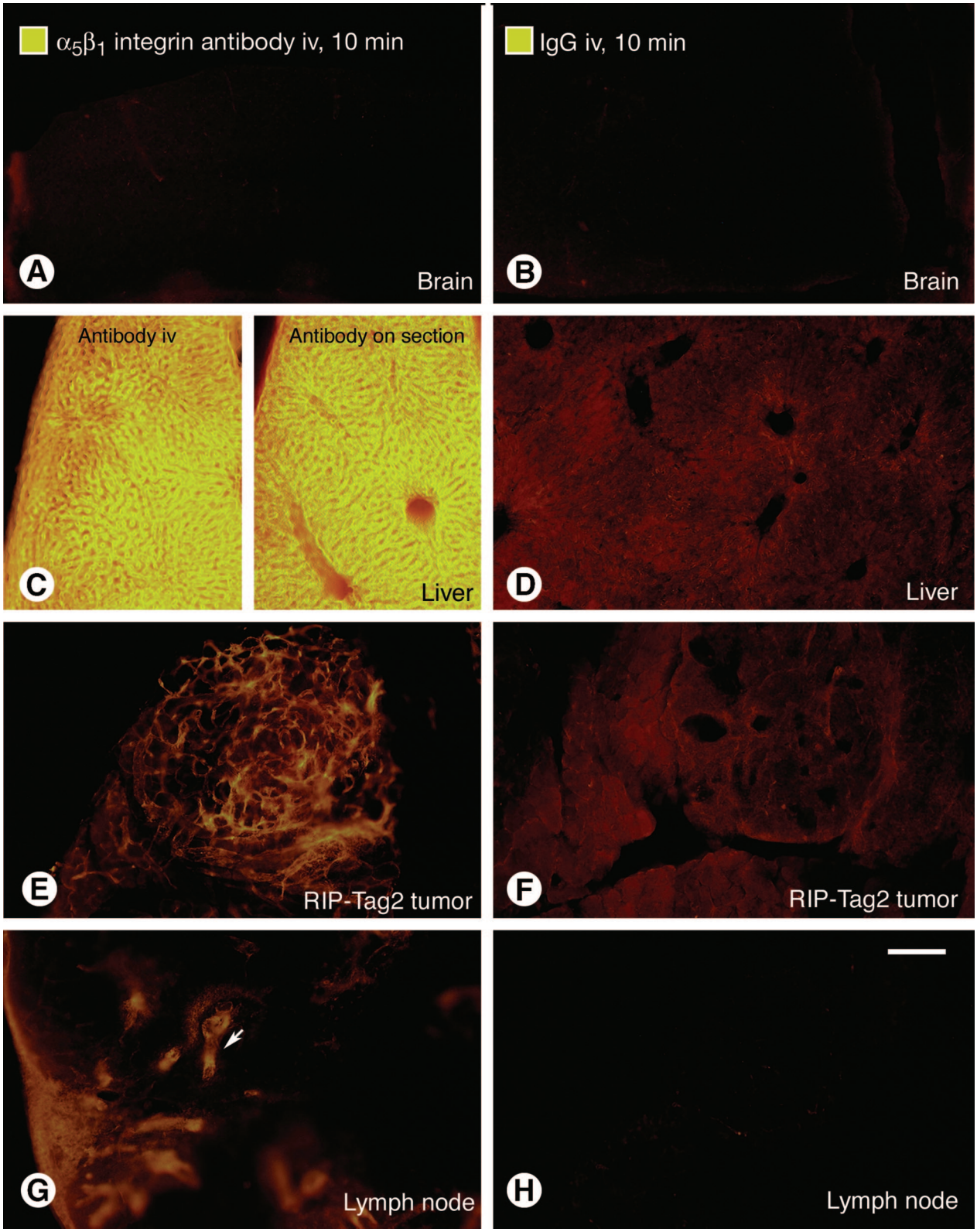

Figure 9. Amount and accessibility of $\alpha_5\beta_1$ integrin in normal organs. Fluorescence micrographs of normal organs and tumors in RIP-Tag2 mice comparing amounts of immunoreactivity at 10 minutes after intravenous injection of anti-$\alpha_5\beta_1$ integrin antibody or nonspecific IgG. All images have various shades of gold because they were obtained with standardized settings of the digital camera optimized for the yellow-orange Cy3 fluorophore attached to the secondary antibody. With these camera settings, no staining is visible in brain after intravenous injection of anti-$\alpha_5\beta_1$ integrin antibody (**A**) or nonspecific IgG (**B**). Liver sinusoids have strong immunoreactivity after intravenous injection of anti-$\alpha_5\beta_1$ integrin antibody (**C**, **left**), and after conventional immunohistochemistry for $\alpha_5\beta_1$ integrin where the antibody is put on the section (**C**, **right**), but not after nonspecific IgG (**D**). For comparison, RIP-Tag2 tumors are shown after injection of anti-$\alpha_5\beta_1$ integrin antibody (**E**) or nonspecific IgG (**F**). High endothelial venules (**arrow**) in mesenteric lymph node have strong immunoreactivity after injection of anti-$\alpha_5\beta_1$ integrin antibody (**G**) but not after nonspecific IgG (**H**). Scale bar, 100 μm.

Table 1. Intensity of Immunofluorescence of Vasculature 10 Minutes after Intravenous Injection of Anti-$\alpha_5\beta_1$ Integrin Antibody or Nonspecific IgG in Mice

	$\alpha_5\beta_1$ Integrin antibody	Nonspecific IgG		$\alpha_5\beta_1$ Integrin antibody	Nonspecific IgG
Liver	+++	+	Pancreatic islets	+	0
Spleen	+++	+	Pancreatic acini	+	0
RIP-Tag2 tumors	++	+	Ileum	+	0
apc tumors	++	+	Skeletal muscle	+	0
MCa-IV tumors	++	+	Brain	0	0
Kidney	++	+	Lung	0	0
Lymph nodes	+	0	Testis	0	0

Values represent the relative intensity of immunofluorescence of normal organs and tumors in mice (n = 3 per group) at 10 minutes after intravenous injection of anti-$\alpha_5\beta_1$ integrin antibody or nonspecific IgG. Digital images of all tissues were obtained at the same camera settings and then ranked by intensity of immunoreactivity, ranging from strongest (+++) to undetectable (0), so overall fluorescence of tumors and normal organs could be meaningfully compared. Fluorescence intensity reflects a combination of abundance of $\alpha_5\beta_1$ integrin-positive blood vessels, strength of immunoreactivity of individual vessels, and amount of antibody extravasation. All three contributed in tumors, but vessel immunoreactivity and abundance dominated in liver, and extravasation dominated in spleen.

lature of MCa-IV tumors has an unusually large (~2000 nm) pore size.[18,20] The presence of focal, patchy accumulations of nonspecific IgG and anti-$\alpha_5\beta_1$ integrin antibody in the interstitium confirmed the leakiness of tumor vessels to macromolecules in all three models we studied. Patchy regions of antibody extravasation were identifiable because they co-localized with fibrin in the stroma[53] and with components of basement membrane and extracellular matrix (unpublished data).[54]

However, most of the intense labeling of tumor vessels by anti-$\alpha_5\beta_1$ integrin antibody is unlikely to simply reflect vascular leakiness. Most anti-$\alpha_5\beta_1$ integrin antibody that accumulated in RIP-Tag2 tumors co-localized with CD31 immunoreactivity, which is known to be expressed by most blood vessels in these tumors and to match the distribution of intravenously injected fluorescent *Lycopersicon esculentum* lectin and four other endothelial cell markers (CD105, VEGFR-2, VEGFR-3, and $\alpha_5\beta_1$ integrin).[30] Unlike the intense, uniform labeling of tumor vessels by the $\alpha_5\beta_1$ integrin antibody, accumulations of nonspecific IgG were patchy, weakly fluorescent, and primarily extravascular. Labeling of tumor vessels by anti-$\alpha_5\beta_1$ integrin antibody is consistent with a uniform vascular expression of the integrin, whereas patchy, extravascular labeling is consistent with the heterogeneous leakiness of tumor vessels.[19,21,22]

Luminal Expression of $\alpha_5\beta_1$ Integrin on Endothelial Cells

Did the anti-$\alpha_5\beta_1$ integrin antibody bind to the luminal or abluminal surface of tumor vessels? Binding to $\alpha_5\beta_1$ integrin on the abluminal surface of endothelial cells or on stromal cells would require intravascular antibodies to cross the endothelial barrier. However, if $\alpha_5\beta_1$ integrin is expressed on the luminal surface of tumor vessels, binding sites would be immediately accessible to antibodies in the bloodstream. In pilot studies, we attempted to determine the location of the labeling by using confocal microscopy and fluorescence microscopy with filters for viewing two fluorophores simultaneously to examine tissue sections of various thicknesses of RIP-Tag2 tumors stained for both $\alpha_5\beta_1$ integrin and CD31 immunoreactivities. Although the approach seemed reasonable, it did not convincingly show whether $\alpha_5\beta_1$ integrin was on the luminal surface, abluminal surface, or both surfaces of endothelial cells (unpublished data). The problem appears to concern the thinness of the endothelial cells compared to the resolution of fluorescence and confocal microscopy. Immunogold labeling for electron microscopy may work, but even that approach will be tricky because the $\alpha_5\beta_1$ integrin antibody leaks into the tumor at some locations. Accumulations at sites of leakage will have to be distinguished from sites of binding.

The location of anti-$\alpha_5\beta_1$ integrin antibody binding was explored further in a companion study by comparing the kinetics of accumulation of antibodies to $\alpha_5\beta_1$ integrin to those of antibodies to three other targets in RIP-Tag2 tumors.[53] During the 24-hour period of that study, the $\alpha_5\beta_1$ integrin antibody maintained its strong, uniform vascular association and also accumulated throughout time at sites of leakage in tumors. By comparison, antibodies to fibronectin, type IV collagen, and fibrin accumulated mainly at sites of leakage. Accumulation of these antibodies was minimal at 10 minutes, peaked at 6 hours, and then plateaued. The half-life of labeling by $\alpha_5\beta_1$ integrin antibody was less than 10 minutes, but the half-life of labeling by the other antibodies was a few hours. Also, the targets were different, with the $\alpha_5\beta_1$ integrin antibody mainly targeting tumor vessels and the others accumulating at sites of leakage. These striking differences in kinetics and distribution add further evidence that $\alpha_5\beta_1$ integrin is expressed on the luminal surface of tumor vessels and fibronectin, type IV collagen, and fibrin are not. Endothelial cells in culture express integrins on both apical and basolateral surfaces.[55] Bacteriophage displaying peptides containing RGD (Arg-Gly-Asp) sequences on their surface rapidly home to tumors by binding to integrins on blood vessels.[56] Similarly, RGD-modified liposomes can target the endothelium of tumor vessels and deliver therapeutic payloads.[16]

Functional Effects of Anti-$\alpha_5\beta_1$ Integrin Antibodies

The functional significance of the rapid accumulation on tumor vessels of $\alpha_5\beta_1$ integrin antibody in the bloodstream cannot be directly tested in mice because of the

lack of availability of function-blocking antibodies with documented functional efficacy *in vivo*. The 5H10-27 anti-α_5 integrin antibody used in the present study inhibits fibronectin binding and cellular migration *in vitro* in systems not involving endothelial cells,[32,33] but has not been shown to affect endothelial cells or angiogenesis *in vivo* and has not been used to inhibit integrin ligation in tumor models.

We found no adverse effects from 10 minutes to 24 hours after injection of the anti-$\alpha_5\beta_1$ integrin antibody, and observed no pathological changes in histological studies of liver and other sites of antibody binding. The absence of functional changes could be a manifestation of absence of blocking action, brief treatment period, dose, or insensitivity to integrin inactivation despite the presence of binding sites for $\alpha_5\beta_1$ integrin antibody. However, the toxicity issue was directly addressed for a potent function-blocking anti-human $\alpha_5\beta_1$ integrin antibody with established anti-angiogenic activity, and the antibody was found to have minimal toxicity in primates.[57] Preclinical studies performed on cynomolgus monkeys show no significant toxicity with doses as large as 50 mg/kg i.v. (unpublished data).[57] Similarly, the antibody has minimal side effects in humans given doses up to 15 mg/kg i.v. in a phase I clinical trial.[25] Antibody 5H10-27 was used in a dose of 2 mg/kg in the present studies.

Integrins as Vascular Targets

Multiple molecular markers have been identified as vascular targets in tumors. Integrin $\alpha_v\beta_3$, which is up-regulated in tumor vessels, is one of the most extensively studied targets for inhibiting and imaging angiogenesis in tumors.[15,44] Tumstatin, a cleavage fragment of the α_3 chain of type IV collagen, appears to inhibit angiogenesis by binding $\alpha_v\beta_3$ integrin, and part of the anti-angiogenic action of endostatin may be mediated by binding $\alpha_5\beta_1$ integrin.[43] Integrin targeting by RGD peptides increases efficacy of doxorubicin and tumor necrosis factor-α in preclinical tumor models.[10,16,58]

The uniform distribution and rapid accessibility of $\alpha_5\beta_1$ integrin on tumor vessels suggest that it would be an effective target for delivery of agents preferentially to blood vessels in tumors. The results of studies using inhibitors of $\alpha_5\beta_1$ integrin on preclinical tumor models support this function.[13,24] The distinctive anatomical distribution and high level of expression of $\alpha_5\beta_1$ integrin warrant further functional studies to explore specificity and efficacy as a target for imaging and therapeutics in cancer.

In conclusion, the results of these experiments taken together show that $\alpha_5\beta_1$ integrin on tumor blood vessels is overexpressed and rapidly accessible to antibodies in the bloodstream. The strong, uniform labeling of tumor vessels by anti-$\alpha_5\beta_1$ integrin antibody circulating in the bloodstream contrasts with weak labeling of most normal blood vessels. The rapid accessibility of the integrin on tumor vessels distinguishes it from most sites of integrin expression outside the vasculature. Because the labeling of $\alpha_5\beta_1$ integrin by intravascular antibody far exceeds the accumulation of nonspecific IgG, abluminal overexpression of integrin combined with vessel leakiness is unlikely to explain the rapid accumulation of anti-integrin antibody in tumors. Overexpression of the integrin on the luminal surface of tumor vessels appears to be a more important factor. Because of these properties, $\alpha_5\beta_1$ integrin has a promising role as a vascular target for antibodies in tumors.

Acknowledgments

We thank Rakesh Jain, Massachusetts General Hospital, Harvard University, for the kind gift of the MCa-IV mouse mammary carcinoma cells; Douglas Hanahan at University of California, San Francisco, for supplying breeding pairs for our colony of RIP-Tag2 mice; Gyulnar Baimukanova for genotyping the mice; Susan Watson, Eos Biotechnology, Inc., for helpful discussions of $\alpha_5\beta_1$ integrin expression in endothelial cells; Barbara Sennino and Tsutomu Nakahara for help with some of the experiments; and Shunichi Morikawa, formerly at University of California, San Francisco, now at Tokyo Women's Medical University, Tokyo, for help with the immunohistochemical staining of tumor vessels.

References

1. Yang JC, Haworth L, Sherry RM, Hwu P, Schwartzentruber DJ, Topalian SL, Steinberg SM, Chen HX, Rosenberg SA: A randomized trial of bevacizumab, an anti-vascular endothelial growth factor antibody, for metastatic renal cancer. N Engl J Med 2003, 349:427–434
2. Hurwitz H, Fehrenbacher L, Novotny W, Cartwright T, Hainsworth J, Heim W, Berlin J, Baron A, Griffing S, Holmgren E, Ferrara N, Fyfe G, Rogers B, Ross R, Kabbinavar F: Bevacizumab plus irinotecan, fluorouracil, and leucovorin for metastatic colorectal cancer. N Engl J Med 2004, 350:2335–2342
3. Yuan F, Chen Y, Dellian M, Safabakhsh N, Ferrara N, Jain RK: Time-dependent vascular regression and permeability changes in established human tumor xenografts induced by an anti-vascular endothelial growth factor/vascular permeability factor antibody. Proc Natl Acad Sci USA 1996, 93:14765–14770
4. Shaheen RM, Davis DW, Liu W, Zebrowski BK, Wilson MR, Bucana CD, McConkey DJ, McMahon G, Ellis LM: Antiangiogenic therapy targeting the tyrosine kinase receptor for vascular endothelial growth factor receptor inhibits the growth of colon cancer liver metastasis and induces tumor and endothelial cell apoptosis. Cancer Res 1999, 59:5412–5416
5. Huang J, Frischer JS, Serur A, Kadenhe A, Yokoi A, McCrudden KW, New T, O'Toole K, Zabski S, Rudge JS, Holash J, Yancopoulos GD, Yamashiro DJ, Kandel JJ: Regression of established tumors and metastases by potent vascular endothelial growth factor blockade. Proc Natl Acad Sci USA 2003, 100:7785–7790
6. Bruns CJ, Liu W, Davis DW, Shaheen RM, McConkey DJ, Wilson MR, Bucana CD, Hicklin DJ, Ellis LM: Vascular endothelial growth factor is an in vivo survival factor for tumor endothelium in a murine model of colorectal carcinoma liver metastases. Cancer 2000, 89:488–499
7. Jain RK: Normalizing tumor vasculature with anti-angiogenic therapy: a new paradigm for combination therapy. Nat Med 2001, 7:987–989
8. Willett CG, Boucher Y, di Tomaso E, Duda DG, Munn LL, Tong RT, Chung DC, Sahani DV, Kalva SP, Kozin SV, Mino M, Cohen KS, Scadden DT, Hartford AC, Fischman AJ, Clark JW, Ryan DP, Zhu AX, Blaszkowsky LS, Chen HX, Shellito PC, Lauwers GY, Jain RK: Direct evidence that the VEGF-specific antibody bevacizumab has antivascular effects in human rectal cancer. Nat Med 2004, 10:145–147
9. St Croix B, Rago C, Velculescu V, Traverso G, Romans KE, Montgomery E, Lal A, Riggins GJ, Lengauer C, Vogelstein B, Kinzler KW:

Genes expressed in human tumor endothelium. Science 2000, 289:1197–1202
10. Arap W, Pasqualini R, Ruoslahti E: Cancer treatment by targeted drug delivery to tumor vasculature in a mouse model. Science 1998, 279:377–380
11. Pasqualini R, Arap W, McDonald DM: Probing the structural and molecular diversity of tumor vasculature. Trends Mol Med 2002, 8:563–571
12. Brooks PC, Clark RA, Cheresh DA: Requirement of vascular integrin alpha v beta 3 for angiogenesis. Science 1994, 264:569–571
13. Kim S, Bell K, Mousa SA, Varner JA: Regulation of angiogenesis in vivo by ligation of integrin alpha5beta1 with the central cell-binding domain of fibronectin. Am J Pathol 2000, 156:1345–1362
14. Kim S, Bakre M, Yin H, Varner JA: Inhibition of endothelial cell survival and angiogenesis by protein kinase A. J Clin Invest 2002, 110:933–941
15. Ruegg C, Mariotti A: Vascular integrins: pleiotropic adhesion and signaling molecules in vascular homeostasis and angiogenesis. Cell Mol Life Sci 2003, 60:1135–1157
16. Schiffelers RM, Koning GA, ten Hagen TL, Fens MH, Schraa AJ, Janssen AP, Kok RJ, Molema G, Storm G: Anti-tumor efficacy of tumor vasculature-targeted liposomal doxorubicin. J Control Release 2003, 91:115–122
17. Dvorak HF, Nagy JA, Dvorak JT, Dvorak AM: Identification and characterization of the blood vessels of solid tumors that are leaky to circulating macromolecules. Am J Pathol 1988, 133:95–109
18. Hobbs SK, Monsky WL, Yuan F, Roberts WG, Griffith L, Torchilin VP, Jain RK: Regulation of transport pathways in tumor vessels: role of tumor type and microenvironment. Proc Natl Acad Sci USA 1998, 95:4607–4612
19. Jain RK: Physiological barriers to delivery of monoclonal antibodies and other macromolecules in tumors. Cancer Res 1990, 50:814s–819s
20. Hashizume H, Baluk P, Morikawa S, McLean JW, Thurston G, Roberge S, Jain RK, McDonald DM: Openings between defective endothelial cells explain tumor vessel leakiness. Am J Pathol 2000, 156:1363–1380
21. Nugent LJ, Jain RK: Extravascular diffusion in normal and neoplastic tissues. Cancer Res 1984, 44:238–244
22. Yuan F, Leunig M, Huang SK, Berk DA, Papahadjopoulos D, Jain RK: Microvascular permeability and interstitial penetration of sterically stabilized (stealth) liposomes in a human tumor xenograft. Cancer Res 1994, 54:3352–3356
23. Ebbinghaus C, Scheuermann J, Neri D, Elia G: Diagnostic and therapeutic applications of recombinant antibodies: targeting the extradomain B of fibronectin, a marker of tumor angiogenesis. Curr Pharm Des 2004, 10:1537–1549
24. Stoeltzing O, Liu W, Reinmuth N, Fan F, Parry GC, Parikh AA, McCarty MF, Bucana CD, Mazar AP, Ellis LM: Inhibition of integrin alpha5beta1 function with a small peptide (ATN-161) plus continuous 5-FU infusion reduces colorectal liver metastases and improves survival in mice. Int J Cancer 2003, 104:496–503
25. Ricart A, Liu G, Tolcher A, Schwartz G, Harris J, Stagg R, Rowinsky E, Wilding G: A phase I dose-escalation study of anti-$\alpha5\beta1$ integrin monoclonal antibody (M200) in patients with refractory solid tumors. Eur J Cancer Suppl 2004, 2:52
26. Hanahan D: Heritable formation of pancreatic beta-cell tumours in transgenic mice expressing recombinant insulin/simian virus 40 oncogenes. Nature 1985, 315:115–122
27. Su LK, Kinzler KW, Vogelstein B, Preisinger AC, Moser AR, Luongo C, Gould KA, Dove WF: Multiple intestinal neoplasia caused by a mutation in the murine homolog of the APC gene. Science 1992, 256:668–670
28. Yang K, Edelmann W, Fan K, Lau K, Kolli VR, Fodde R, Khan PM, Kucherlapati R, Lipkin M: A mouse model of human familial adenomatous polyposis. J Exp Zool 1997, 277:245–254
29. McDonald DM, Choyke PL: Imaging of angiogenesis: from microscope to clinic. Nat Med 2003, 9:713–725
30. Inai T, Mancuso M, Hashizume H, Baffert F, Haskell A, Baluk P, Hu-Lowe DD, Shalinsky DR, Thurston G, Yancopoulos GD, McDonald DM: Inhibition of vascular endothelial growth factor (VEGF) signaling in cancer causes loss of endothelial fenestrations, regression of tumor vessels, and appearance of basement membrane ghosts. Am J Pathol 2004, 165:35–52
31. Zlotecki RA, Boucher Y, Lee I, Baxter LT, Jain RK: Effect of angiotensin II induced hypertension on tumor blood flow and interstitial fluid pressure. Cancer Res 1993, 53:2466–2468
32. Schultz JF, Armant DR: Beta 1- and beta 3-class integrins mediate fibronectin binding activity at the surface of developing mouse peri-implantation blastocysts. Regulation by ligand-induced mobilization of stored receptor. J Biol Chem 1995, 270:11522–11531
33. Ruppert M, Aigner S, Hubbe M, Yagita H, Altevogt P: The L1 adhesion molecule is a cellular ligand for VLA-5. J Cell Biol 1995, 131:1881–1891
34. Joyce NC, Haire MF, Palade GE: Morphologic and biochemical evidence for a contractile cell network within the rat intestinal mucosa. Gastroenterology 1987, 92:68–81
35. Yang JT, Rayburn H, Hynes RO: Embryonic mesodermal defects in alpha 5 integrin-deficient mice. Development 1993, 119:1093–1105
36. George EL, Georges-Labouesse EN, Patel-King RS, Rayburn H, Hynes RO: Defects in mesoderm, neural tube and vascular development in mouse embryos lacking fibronectin. Development 1993, 119:1079–1091
37. Francis SE, Goh KL, Hodivala-Dilke K, Bader BL, Stark M, Davidson D, Hynes RO: Central roles of alpha5beta1 integrin and fibronectin in vascular development in mouse embryos and embryoid bodies. Arterioscler Thromb Vasc Biol 2002, 22:927–933
38. van Vliet AI, van Alderwegen IE, Baelde HJ, de Heer E, Bruijn JA: Fibronectin accumulation in glomerulosclerotic lesions: self-assembly sites and the heparin II binding domain. Kidney Int 2002, 61:481–489
39. Boudreau NJ, Varner JA: The homeobox transcription factor Hox D3 promotes integrin alpha5beta1 expression and function during angiogenesis. J Biol Chem 2004, 279:4862–4868
40. Collo G, Pepper MS: Endothelial cell integrin alpha5beta1 expression is modulated by cytokines and during migration in vitro. J Cell Sci 1999, 112:569–578
41. Suehiro K, Gailit J, Plow EF: Fibrinogen is a ligand for integrin alpha5beta1 on endothelial cells. J Biol Chem 1997, 272:5360–5366
42. Suehiro K, Mizuguchi J, Nishiyama K, Iwanaga S, Farrell DH, Ohtaki S: Fibrinogen binds to integrin alpha(5)beta(1) via the carboxyl-terminal RGD site of the Aalpha-chain. J Biochem (Tokyo) 2000, 128:705–710
43. Sudhakar A, Sugimoto H, Yang C, Lively J, Zeisberg M, Kalluri R: Human tumstatin and human endostatin exhibit distinct antiangiogenic activities mediated by alpha v beta 3 and alpha 5 beta 1 integrins. Proc Natl Acad Sci USA 2003, 100:4766–4771
44. Brooks PC, Montgomery AM, Rosenfeld M, Reisfeld RA, Hu T, Klier G, Cheresh DA: Integrin alpha v beta 3 antagonists promote tumor regression by inducing apoptosis of angiogenic blood vessels. Cell 1994, 79:1157–1164
45. Mitjans F, Meyer T, Fittschen C, Goodman S, Jonczyk A, Marshall JF, Reyes G, Piulats J: In vivo therapy of malignant melanoma by means of antagonists of alphav integrins. Int J Cancer 2000, 87:716–723
46. Meerovitch K, Bergeron F, Leblond L, Grouix B, Poirier C, Bubenik M, Chan L, Gourdeau H, Bowlin T, Attardo G: A novel RGD antagonist that targets both alphavbeta3 and alpha5beta1 induces apoptosis of angiogenic endothelial cells on type I collagen. Vascul Pharmacol 2003, 40:77–89
47. Sincock PM, Mayrhofer G, Ashman LK: Localization of the transmembrane 4 superfamily (TM4SF) member PETA-3 (CD151) in normal human tissues: comparison with CD9, CD63, and alpha5beta1 integrin. J Histochem Cytochem 1997, 45:515–525
48. Cheuk BL, Cheng SW: Differential expression of integrin alpha5beta1 in human abdominal aortic aneurysm and healthy aortic tissues and its significance in pathogenesis. J Surg Res 2004, 118:176–182
49. Hynes RO: Fibronectins. New York, Springer-Verlag, 1990
50. Taverna D, Hynes RO: Reduced blood vessel formation and tumor growth in alpha5-integrin-negative teratocarcinomas and embryoid bodies. Cancer Res 2001, 61:5255–5261
51. Ritter MR, Dorrell MI, Edmonds J, Friedlander SF, Friedlander M: Insulin-like growth factor 2 and potential regulators of hemangioma growth and involution identified by large-scale expression analysis. Proc Natl Acad Sci USA 2002, 99:7455–7460
52. McDonald DM, Baluk P: Significance of blood vessel leakiness in cancer. Cancer Res 2002, 62:5381–5385
53. Magnussen A, Kasman IM, Norberg S, Baluk P, Murray R, McDonald DM: Rapid access of antibodies to alpha5beta1 integrin overexpressed

on the luminal surface of tumor blood vessels. Cancer Res 2005, 65:2712–2721
54. Baluk P, Morikawa S, Haskell A, Mancuso M, McDonald DM: Abnormalities of basement membrane on blood vessels and endothelial sprouts in tumors. Am J Pathol 2003, 163:1801–1815
55. Conforti G, Dominguez-Jimenez C, Zanetti A, Gimbrone Jr MA, Cremona O, Marchisio PC, Dejana E: Human endothelial cells express integrin receptors on the luminal aspect of their membrane. Blood 1992, 80:437–446
56. Pasqualini R, Koivunen E, Ruoslahti E: Alpha v integrins as receptors for tumor targeting by circulating ligands. Nat Biotechnol 1997, 15:542–546
57. Ramakrishnan V, Johnson D, Wills M, Law D, Daly R, Wong M, Castillo A, O'Hara C, Hevezi P, Powers D, DuBridge R, Caras I, Wright M, Fang Y, Finck B, Murray R, Jeffry U: A function blocking chimeric antibody, Eos200-4, against a5b1 integrin inhibits angiogenesis in a monkey model. Proc Am Assoc Cancer Res 2003, 44:A3052
58. Curnis F, Gasparri A, Sacchi A, Longhi R, Corti A: Coupling tumor necrosis factor-alpha with alphaV integrin ligands improves its antineoplastic activity. Cancer Res 2004, 64:565–571